

# FH Aachen

## Faculty Electrical Engineering and Information Technology

### Information Systems Engineering

Master Thesis

#### **Development of a hardware and software framework for the automated characterization of permanent magnets for low-field MRI systems**

Submitted by

**Marcel Werner Heinrich Friedrich Ochsendorf**

Matriculation number: **3120232**

Examiner:

Prof. Dr.-Ing. Thomas Dey

Examiner:

Prof. Dr.-Ing. Volkmar Schulz

Date:

15.01.2024

# **Erklärung**

Hiermit versichere ich, dass ich die vorliegende Arbeit selbstständig verfasst und keine anderen als die im Literaturverzeichnis angegebenen Quellen benutzt habe. Stellen, die wörtlich oder sinngemäß aus veröffentlichten oder noch nicht veröffentlichten Quellen entnommen sind, sind als solche kenntlich gemacht. Die Zeichnungen oder Abbildungen in dieser Arbeit sind von mir selbst erstellt worden oder mit einem entsprechenden Nachweis versehen. Diese Arbeit ist in gleicher oder ähnlicher Form noch bei keiner anderen Prüfungsbehörde eingereicht worden.

Aachen, \_\_\_\_\_, \_\_\_\_\_

# Abstract

A large number of permanent magnets are used in the construction of low-field MRI equipment on the basis of permanent magnets. The magnetic properties of these magnets must be similar to a certain degree in order to achieve a homogeneous  $B_0$  field, which is necessary for many setups.

Due to the complex manufacturing process of neodymium magnets, the different properties, i.e. the direction of magnetisation, can deviate from each other. This affects the homogeneity of the field and the image acquisition.

A passive shimming process is typically used to adjust the field afterwards. This is complex and time-consuming and requires manual corrections to the magnets used. To avoid this process, magnets can be systematically measured in advance. Sensor accuracy and repeatability Data acquisition, storage and subsequent analysis play an important role in this methodology.

Several existing open source solutions implement individual parts, but do not provide a complete data processing pipeline from acquisition to analysis, and their data storage formats are not compatible with each other.

For this use case, the MagneticReadoutProcessing library has been created in this work. It implements all important aspects of acquisition, storage and analysis, and each intermediate step can be customised by the user without having to create everything from scratch, thus encouraging exchange between different user groups.

Complete documentation, tutorials and tests enable users to use and adapt the framework as quickly as possible. The framework was used to characterise different magnets, which requires integrating magnetic field sensors.

To evaluate the software framework and hardware, two digital sensors were characterised and tested under the same conditions for noise, temperature dependence and linearity. The result is that both sensors can only be used under certain conditions, as the noise intensity is higher than the specified  $50 \mu\text{T}$  and the value ranges fluctuate too much as a result. It is recommended to consider analogue sensors or NMR probes in the future.



# List of abbreviations

**CAD** Computer Aided Design. 4, 9, 17, 32–34

**CDC** Communication Device Class. 20

**CLI** Command Line Interface. 21, 22, 25, 41, 43, 44, 51, 53–55, 61, 65, 69

**GPIO** General Purpose Input/Output. 18, 24, 29

**GUI** Graphical User Interface. 53

**HAL** Hardware Abstraction Layer. 22, 37, 41

**HTML** Hypertext Markup Language. 62

**I2C** Inter-Integrated Circuit. 16, 20

**IC** Integrated Circuit. 17, 18, 76, 78, 81

**ID** Identification Number. 70

**IDE** Integrated Development Environment. 58, 62

**IP** Internet Protocol. 42

**JSON** JavaScript Object Notation. 32, 36, 37, 46

**LUT** Lookup Table. 20, 43, 44

**MRI** Magnetic Resonance Imaging. 1–4, 6, 7, 9, 32, 33, 49

**MRP** MagneticReadoutProcessing. 15, 21–24, 43, 45, 48, 53, 55, 58–62, 64, 88

**NMR** Nuclear Magnetic Resonance. 1, 4, 6

**OS** Operating System. 23

**PC** Personal Computer. 15, 18–22, 29, 30, 39–43, 46, 54, 59, 60, 81

**PCB** Printed Circuit Board. 18

**PDF** Portable Document Format. 62

**PIP** Python Package Installer. 60

**ppm** Parts Per Million. 3, 7, 9–11, 71, 84, 85

**PPS** Puls Per Second. 42

**PTP** Precision Time Protocol. 42

**REST** Representational State Transfer. 39, 41

**SBC** Single Board Computer. 23, 29, 39, 42

**SD** Standard deviation. 75, 76, 79, 84

**SNR** Signal to Noise Ratio. 3, 4

**UART** Universal Asynchronous Receiver / Transmitter. 20, 29

**USB** Universal Serial Bus. 20, 22, 23, 38, 42, 74

**UUID** Universal Unique Identifier. 24, 37, 43–45, 47

# Contents

<b>1</b>	<b>Introduction</b>	<b>1</b>
1.1	Background and Motivation . . . . .	1
1.1.1	Low-Field MRI . . . . .	3
1.1.2	Magnet System . . . . .	4
1.1.3	Shimming Procedure . . . . .	6
1.2	State of the Art . . . . .	7
1.3	Aim of this Thesis . . . . .	9
1.4	Research Question and Approach . . . . .	10
1.5	Usecases . . . . .	12
1.6	Structure . . . . .	13
<b>2</b>	<b>Unified Sensor</b>	<b>15</b>
2.1	Sensor Selection . . . . .	15
2.2	Mechanical Structure . . . . .	17
2.3	Electrical Interface . . . . .	18
2.4	Firmware . . . . .	19
2.4.1	Communication Interface . . . . .	21
2.4.2	Sensor Syncronisation Interface . . . . .	22
2.5	Example Sensors . . . . .	24
2.5.1	1D: Single Sensor . . . . .	27
2.5.2	3D: Full Sphere . . . . .	27
2.5.3	Integration of an Industry-Teslameter . . . . .	29
<b>3</b>	<b>Software Readout Framework</b>	<b>31</b>
3.1	User Interaction Points . . . . .	31
3.1.1	User Interaction Points Example . . . . .	32
3.2	Modules . . . . .	34
3.2.1	Core Modules . . . . .	34
3.2.2	Storage and Datamanagement . . . . .	35
3.2.3	Extension Modules . . . . .	37

3.3	Multi Sensor Setup . . . . .	39
3.3.1	Network-Proxy . . . . .	41
3.3.2	Sensor Syncronisation . . . . .	42
3.3.3	Command-Router . . . . .	43
3.4	Examples . . . . .	45
3.4.1	MRPReading . . . . .	45
3.4.2	MRPHal . . . . .	46
3.4.3	MRPSimulation . . . . .	47
3.4.4	MRPAnalysis . . . . .	48
3.4.5	MRPVisualisation . . . . .	49
3.4.6	MRPHalbachArrayGenerator . . . . .	49
<b>4</b>	<b>Usability Improvements</b>	<b>53</b>
4.1	Command Line Interface . . . . .	53
4.2	Programmable Data Processing Pipeline . . . . .	55
4.3	Testing . . . . .	58
4.4	Package Distribution . . . . .	60
4.4.1	Documentation . . . . .	62
<b>5</b>	<b>UseCase Evaluation</b>	<b>64</b>
5.1	Hardware preparation . . . . .	65
5.2	Configuration of the Measurement . . . . .	65
5.3	Custom Algorithm Implementation . . . . .	66
5.3.1	Alternative Filter Algorithm Implementation . . . . .	67
5.4	Execution of Analysis Pipeline . . . . .	68
5.5	Result Analysis . . . . .	69
<b>6</b>	<b>Evaluation</b>	<b>71</b>
6.1	Sensors for Evaluation . . . . .	71
6.2	Evaluation Sensor Setup . . . . .	73
6.3	Sensor Characterisation: Background-Noise . . . . .	74
6.3.1	Sensor Temperature Analysis . . . . .	76
6.3.2	Raw Sensor Data Analysis . . . . .	76
6.4	Sensor Characterisation: Linearity . . . . .	78
6.4.1	Measurement Setup . . . . .	78
6.4.2	Measurement Run . . . . .	79
6.4.3	Linearity Analysis . . . . .	79
6.5	Sensor Characterisation: Temperature Sensitivity . . . . .	81
6.5.1	Temperature Sensitivity Analysis . . . . .	82

6.6 Result Analysis . . . . .	82
6.6.1 Recommendation for Action . . . . .	85
<b>7 Conclusion and Discussion</b>	<b>87</b>
7.1 Conclusion . . . . .	87
7.2 Outlook . . . . .	87
<b>Bibliography</b>	<b>89</b>
<b>List of Figures</b>	<b>93</b>
<b>List of Tables</b>	<b>95</b>
<b>Listings</b>	<b>96</b>

# 1 Introduction

As the following, the motivation for the development of this framework is listed. The chapter provides a brief introduction into the problem domain, delineates the scope and boundaries of the present research, surveys the current state of the art in low-field Magnetic Resonance Imaging (MRI) research and applications, articulates the research question driving this thesis and delineates the anticipated usecases and benefits that will be explored and analysed throughout the study.

## 1.1 Background and Motivation

Magnetic Resonance Imaging MRI stands as a cornerstone in clinical diagnostics, utilizing the principles of nuclear magnetic resonance Nuclear Magnetic Resonance (NMR) to generate cross-sectional black-and-white images of the body. This indispensable method plays a central role in contemporary medicine and research, contributing significantly to saving lives. Despite its widespread use, traditional MRI systems often rely on large, heavy, and expensive magnets to achieve the necessary homogeneity of the magnetic field for accurate imaging. [20]

Various types of magnets are applied in different MRI systems. Permanent magnets generate a steady yet relatively weak magnetic field, electro magnets are energized by electrical currents, and superconducting electro magnets produce magnetic fields through electric induction. Regardless of the type, the primary objective is to create a homogeneous magnetic field within the MRI. The higher the homogeneity, the more accurate the measurements. This uniform magnetic field aligns the molecules within the body or object, setting the stage for a second magnetic system to stimulate these molecules for spin-measurements.

The challenge with conventional homogeneity systems lies in their substantial size, weight, and cost. Even when targeting smaller areas of the body, large devices are often

necessary.

In response to this, there is a growing interest in developing low-field MRI systems that utilize in many cases permanent magnets. These systems, while offering advantages in energy efficiency and reduced complexity, face a significant challenge related to the inherent variability in the strength of permanent magnets. Achieving homogeneity in the magnetic field is crucial for accurate imaging or comparative analyses. While typically calculated images have lower resolution due to lower magnetic field strength, low-field systems facilitate the comparison of different field behaviours and the identification of all kinds of irritations. O'Reilly and Teeuwisse and de Gans [22] have already demonstrated low-cost and small-scale implementations with low-field MRI in 2021 calculating images of a head successfully.

Permanent magnets, usually arranged in a circular “Halbach array” inside the MRI, are commonly used in low-field systems. However, their drawback is the inherent variability in strength, complicating the achievement of a homogeneous field and requiring precise strength information for correct magnet ordering and MRI construction.

Completed MRI systems pose significant challenges for retrospective adjustments, particularly when individual magnets impact the overall homogeneity of the magnetic field. While deviations in homogeneity can be measured post-assembly, the intricate task of readjustment is taken into account. It is less cost-intensive and less complicated to measure the magnets proactively, prior to the finalization of the MRI system.

The focus of this thesis is to improve low-frequency MRI technology by examining the usability of magnetic field sensors for characterising permanent magnets used in these systems. The variability in the strength of permanent magnets leads to significant difficulties in constructing an MRI with the necessary precision for homogenous field generation.

To address this challenge, the thesis proposes the development of a comprehensive hardware and software framework. The hardware system aims to selectively measure magnetic fields at different locations or fully around a permanent magnet using different sensors. Several existing open-source software solutions implement individual parts, but do not provide a complete data processing pipeline from acquisition to analysis, and their data storage formats are not compatible with each other.

The accompanying open-source software for this thesis is designed not only to facilitate measurements with different sensors but also to enable the characterisation of different

objects.

The sensor testing process involves three key test procedures for two digital sensors. Firstly, the background noise for both sensors is quantified by measuring with the sensors in a constant environment without any magnets. Secondly, the linearity of the magnetic fields is measured for all sensors to detect deviations from the estimated ideal magnetic curve.

At last, the temperature drift is measured by repeating the background noise test in different temperature environments. Sensor noise should be less than  $50\mu T$  to characterise precisely a magnetic field in a Halbach-Array of an MRI with precision greater than *1000 Parts Per Million (ppm)*.

This research initiative contributes to the improvement of low-frequency MRI systems by enhancing the accuracy of permanent magnet characterisation. The outcomes of this thesis provides insights into the selection and evaluation of sensors for future low-field MRI research, ultimately contributing to advancements in medical imaging technologies.

### **1.1.1 Low-Field MRI**

For modern medical imaging high-field superconducting magnets dominate most MRI machines, providing high black-with image resolution. However, the substantial costs, space requirements and safety considerations cause considerable challenges.

MRI relies on the presence of a robust magnetic field, and over time, there has been a continual push to enhance the strength of these magnetic fields. This strength is quantified in units of Tesla [T], commonly referred to as the  $B_0$  field in medical contexts, while physicists use the term magnetic field induction. The Signal to Noise Ratio (SNR) is proportional to the magnetic  $B_0$  field; growing magnetic field leads automatically to higher SNR. The initial  $B_0$  field of an MRI aims to be homogeneous, for image acquisition the second step requires inhomogeneity of the  $B_0$  field to stimulate spin in the atoms of materials. For high resolution images, the initial  $B_0$  field aims to be a homogeneous as possible.

Notably, the focus on high-field systems dominated discussions until around 1991 when the possibility of constructing MRI machines with lower magnetic field strengths came

up. This marked a shift in exploring the potential advantages and applications of low-field MRI systems. [20]

Low-field magnetic resonance imaging (low-field MRI) is a MRI technique that operates at a lower magnetic field strength compared to conventional high-field MRI scanners. Typically, the magnetic field in low-field MRI-systems measured between  $0.1T$  and  $0.3T$  compared to the usual  $1.5T$  to  $3T$  and above in high-field MRI scanners [17].

This technology is used in medical imaging as well as in preclinical research. The main advantage of low-field MRIs is the improved imaging of soft material, especially when examining joints and muscles. It also offers more cost-effective alternatives to high-field MRI systems [17], cost reduction, a smaller device footprint, alleviated safety concerns and leading to diminished image resolution within clinically feasible scan durations. [1]

Low-field MRI systems are predominantly composed of permanent magnets. Through the connection of these permanent magnets, a consistent magnetic field of up to  $0.35T$  can be generated. However, this achievement comes at the cost of an average system weight of  $14t$ . Despite their cost-effectiveness in production and maintenance, permanent magnets show drawbacks such as high temperature dependence and a limited SNR due to the constrained field strength. [20]

In particular, the advantages of the small design, the fast and simple image acquisition and the low costs are advantages that will become increasingly important in the future. However, the use of permanent magnets and their structure is particularly important in such systems and needs to be analysed.

### **1.1.2 Magnet System**

The positioning of permanent magnets holds an important role in constructing an MRI and is influencing the homogeneity of the  $B_0$  magnetic field. Halbach ring magnets [15] have become a common design for low field MRI and NMR systems [27].

This positioning has the ability to generate extremely homogeneous magnetic flux densities, produce virtually no stray fields and is particularly attractive for larger magnets as their design has the best flux-to-mass ratio [30].

A Halbach ring of this type is usually based on a ring with permanent magnets arranged in a circle. The graphic 1-1 shows an example Computer Aided Design (CAD) model of

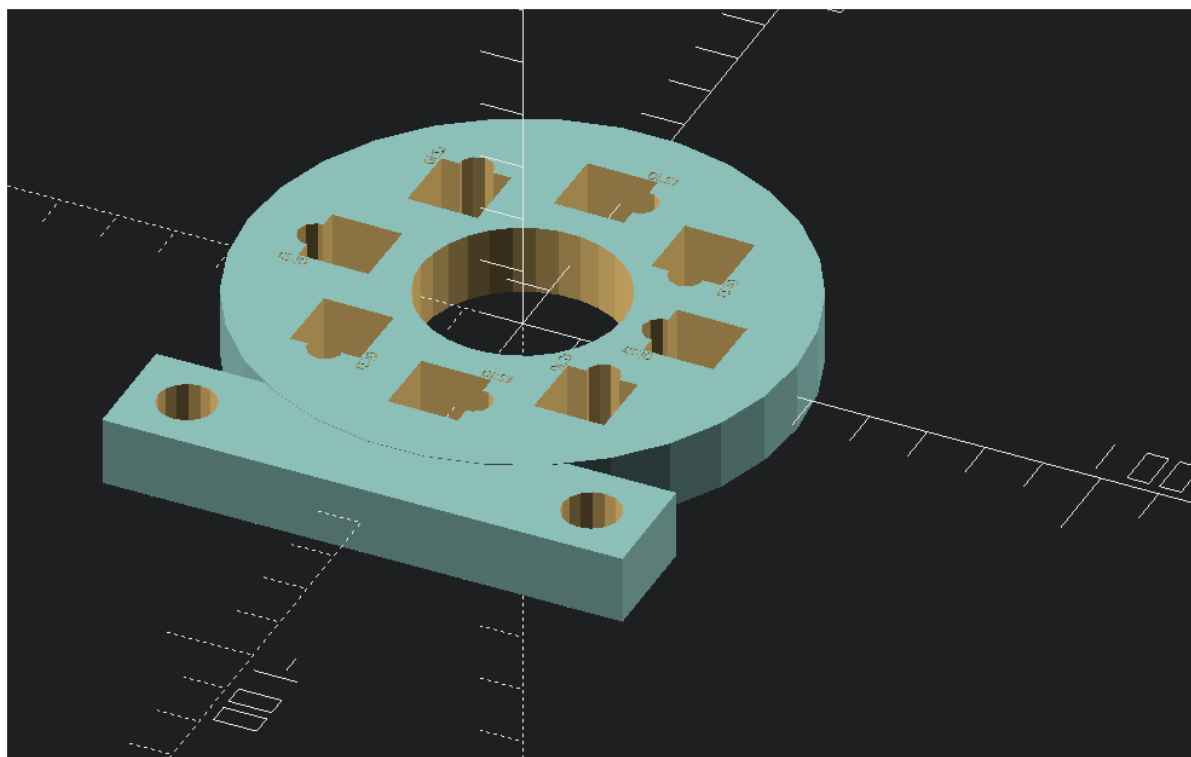


Figure 1-1: Example Hallbach ring with cutouts for eight magnets

such a ring, in which in this case eight cubic  $12 \times 12 \times 12\text{mm}$  magnets are embedded to generate homogeneous magnetic flux densities of around  $20\text{mT}$ .

The homogeneity in this configuration depends, among other things, on the following main aspects:

- **Material:** The magnetic properties of a material influence the generated field strength. Different materials have different magnetic susceptibilities.
- **Magnetization:** The orientation of the magnetic moments in the material influences the field strength. A higher magnetization leads to a stronger field strength.
- **Temperature:** Temperature can influence the magnetic properties of a material. The magnetization of some materials decreases with increasing temperature.
- **Manufacturing process:** The manufacturing process can influence the magnetic properties of the material. This is dependent on the purity of the starting materials used and the processing methods. There may also be deviations in field strength if different magnets from different production batches are compared. [3]

These aspects can also be applied to individual magnets. As a result, this also compli-

cates the effect on the structure of a Halbach ring magnet. If these are joined together to form a ring, positioning tolerances are also added.

Halbach magnetic arrays present a choice for mobile NMR due to their ability to produce highly homogeneous and robust magnetic fields per unit of magnetic mass, coupled with minimal stray fields. The term “Halbach Array” (commonly known as “magic rings”) denotes a precise configuration of permanent magnets designed to amplify magnetic flux on one side while concurrently mitigating or eliminating it on the opposite side. [3]

The Halbach magnetic array appears as a essential element for future Magnet characterisation. Based on this fact this thesis centres on assessing the sensors’ applicability, the Halbach magnetic array serves as a tool for later measurements, although its implementation and further discussion will not be the primary focus.

In order to compensate for inhomogeneities in a finished system, there are various so-called shimming procedures which further improve homogeneity after the system has been assembled. This procedure is explained in the following chapter.

### **1.1.3 Shimming Procedure**

The shimming process is a essential step in magnetic resonance imaging MRI to ensure homogeneous magnetic fields for precise imaging. Shimming corrects irregularities in the static magnetic field that can be caused by external influences or internal system errors. This process optimizes field homogeneity, which is essential for high-resolution and artifact-free images [29].

Optimal homogeneity is attained through intricate designs facilitating active shimming, a technique essential for achieving high-resolution spectroscopy. Beyond this, simpler combinations and adaptations of Halbach rings offer versatility, making them suitable for variable field magnets or magnets that can be effortlessly opened without applying force. [3]

The sources for the shimming process can be hardware and software based. Hardware shimming involves the use of gradient and radio frequency coils that are specifically placed to align the magnetic field. Software shimming, on the other hand, uses algorithms to adjust the control parameters of the MRI system and improve homogeneity [29].

In this thesis, reference is made exclusively to the hardware shimming processes, since

this project is to be used in the future to construct a low-field MRI field magnet from permanent magnets.

## 1.2 State of the Art

### Low-Field MRI

According to Wolfgang R. Nitz in 2016, just 13.4% of actively used MRI systems are low-field MRI (*66.6% 1.5T systems, 20% 3.0 T system, 14.4% low field with <0.5T*). [20]

Within the research domain, various implementations have emerged. An exemplar instance is the work by O'Reilly, Teeuwisse, and Webb, who introduced a groundbreaking “three-dimensional MRI in a homogeneous 27cm diameter Bore Halbach Array magnet” [22] in 2019. This innovative setup is subsequently employed in 2020 to acquire *in vivo* MR images, showcasing the practical applications of their pioneering research [24]. In 2023, de Vos, Remis and Webb published a summary of the design of a point-of-care Halbach array low-field MRI system [28].

Within the research domain, various implementations came up. An exemplar instance is the work by O'Reilly, Teeuwisse, and Webb, who introduced a groundbreaking “three-dimensional MRI in a homogeneous 27cm diameter Bore Halbach Array magnet” [22] in 2019. This innovative setup is subsequently employed in 2020 to acquire *in vivo* MR images, showcasing the practical applications of their pioneering research [24]. In 2023, de Vos, Remis and Webb published a summary of the design of an oint-of-care halbach array low-field MRI system [28].

The Halbach magnet incorporated in this system boasts a 27cm diameter, a  $B_0$  field strength of 50.4mT, and an impressive homogeneity of 2400ppm over a 20cm diameter using smaller magnets ( $12 \times 12 \times 12 \text{ mm}^3$ ). This exceptional homogeneity enables the utilization of coil-based gradients for spatial encoding, significantly enhancing the flexibility of image acquisition.

The Halbach magnet incorporated in this system boasts a 27cm diameter, a  $B_0$  field strength of 50.4 mT, and an impressive homogeneity of 2400ppm over a 20cm diameter using smaller magnets ( $12 \times 12 \times 12 \text{ mm}^3$ ). This exceptional homogeneity enables the utilization of coil-based gradients for spatial encoding, significantly enhancing the

flexibility of image acquisition.

To further refine the magnet's homogeneity, optimisation techniques are employed by adjusting the radius of the Halbach ring along the length of the magnet. The deliberate choice of smaller magnets, as opposed to other Halbach designs, serves to compensate for inherent manufacturing imperfections in each individual magnet. This strategic decision not only mitigates structural demands on the magnet housing in terms of strength and weight but also augments safety throughout the construction process.

## **Magnet Characterisation**

The shimming process described describes how, after the field magnet has been set up, if the homogeneous magnetic flux densities are not sufficient, these can be adjusted manually by means of adjustments to the setup or, if the hardware allows it, by software. In addition, the causes that cause the inhomogeneity, the output permanent magnet, are also known. As a result, there is the possibility of using the shimming process or checking the permanent magnets used in advance before they are used in a Halbach configuration.

In order to measure the magnets individually, there are already implementations that use different measurement methods to determine the field strength of individual magnets and individual measuring points are recorded. This data is then evaluated in separate software [30].

There are two ways of using the data from the magnets that were previously measured:

- By using binning or sorting algorithms to filter for the most similar magnets
- Adjustment of the rotation and position within the Halbach configuration

This form of data processing of previously characterised magnetic data is currently being implemented experimentally in projects using various algorithms [30]. Standard sorting algorithms are used as well as specialized algorithms for optimizing homogeneity by rotating the individual magnets in a Halbach ring relative to each other [2].

These are each separate projects that implement individual aspects of data processing, which realize the process of measuring individual magnets by manual combination. However, there are still compatibility problems and limitations in the adaptation of hardware and software.

Special algorithms from various projects are used to optimize homogeneity. The challenge here is to ensure the seamless integration and compatibility of these algorithms into the overall process. This should make it possible to create a workflow from the individual magnet to the finished optimized CAD model of a halbach ring.

## 1.3 Aim of this Thesis

The present work aims to provide an efficient and comprehensive solution for the design of low-field MRI devices by developing and implementing a software and hardware framework.

Within the framework of the *DeLoRI* (Dedicated Low-field MRI for breast) project, *Fraunhofer MEVIS* in Bremen is actively engaged in crafting a compact and mobile low-field MRI unit customised specifically for screening purposes. As described before, since 1991 low-field MRIs have evolved into a growing realm of research, showcasing significant opportunities within the field of medical technology. The efforts by *Fraunhofer MEVIS* exemplifies the ongoing commitment to utilizing the potential of low-field MRI for enhanced breast screening applications.

The focus of the ongoing efforts is to improve the homogeneity of magnets within low-field MRI systems below 1000ppm, primarily driven by the goal of establishing a compact low-field MRI for breast cancer detection.

Beyond the development and prototype construction of low-field MRI scanners, the project encompasses electromagnetic simulation of components within the low-field MRI system, coupled with machine learning-driven control and data acquisition. The resultant software will be instrumental in reconstruction, with a specific focus on leveraging AI-based methodologies.

This comprehensive effort serves to bolster the prototyping phase of the low-field MRI. Diverging from the approach implemented by O'Reilly, Teeuwisse, and Webb, *DeLoRI* aims to design an open MRI, departing from the circular MRI configuration discussed in the publication. This innovation is geared towards streamlining breast examinations, offering enhanced accessibility, and minimizing the spatial requirements during installation.

In addition *DeLoRI* efforts to achieve heightened accuracy, striving for precision levels

below 1000ppm. While O'Reilly, Teeuwisse, and Webb were able to modify the ring diameter to influence field homogeneity, the unique goal here is to characterize the magnets pre-installation, allowing for proactive assessments of homogeneity characteristics. This approach aims to provide insights into magnetic field uniformity before the magnets are integrated, thereby streamlining the optimisation process. Furthermore,

It is important to note that the primary objective of this thesis is not merely to characterize the magnet itself; rather, the emphasis lies in the selection and comparison of potential sensors for the characterisation process.

To achieve this, a versatile hardware setup is in development, designed to accommodate various sensors for the measurement of magnets or other objects. Simultaneously, a software interface is being crafted to universally read data from different sensors and interact seamlessly with the diverse firmware associated with various Halbach sensors. A key feature of this system is the ease of sensor interchangeability, facilitating adaptability and versatility in the characterisation process.

The scope of the software library is to lay the foundation for the systematic characterisation of magnets based on permanent magnets. The library will enable data acquisition, storage and analysis of magnetic properties, with customisation possible at each step of the process. Complete documentation, tutorials and tests will enable users to use the framework efficiently and adapt it to their specific requirements.

The application of the developed framework for the characterisation of different magnets and the integration of various available magnetic field sensors serve the practical application and validation of the developed solution.

Two sensors have been meticulously chosen for inclusion in the study. The ultimate objective is to assess whether these selected sensors align with the stringent criteria of achieving an accuracy level of 1000ppm. Furthermore, the study seeks to validate whether the measuring range of these sensors appropriately corresponds to the required field strength, ensuring their suitability for the intended application.

## **1.4 Research Question and Approach**

Concerning the *DeLoRI* project, this study exclusively delves into the realm of permanent magnets employed for creating a homogeneous  $B_0$  field through Halbach rings.

Other systems and spin generation for measurements are deliberately excluded from consideration but will be necessary in later stages of the *DeLoRI* project.

Before naming the research focus, it is important to understand the difference and connection between deviation and resolution of the system. To measure a deviation of better than 1000ppm in a 50mT magnetic field, a resolution that is less than 1000ppm of 50mT is needed.

$$\frac{1000}{1000000} \times 50 \text{ mT} = 0.05 \text{ mT}$$

To convert this into microtesla ( $\mu\text{T}$ ), a multiplication by 1000 is needed:

$$0.05 \text{ mT} \times 1000 = 50 \mu\text{T}$$

This means that to measure a deviation of better than 1000ppm in a 50mT magnetic field, a resolution of less than 50  $\mu\text{T}$  is needed.

The primary objectives of this work revolve around addressing two pivotal research questions:

- Sensor characterisation: Can the carefully selected sensors effectively measure a magnet? Specifically, this involves investigating the saturation of the sensors, the linearity of field strength concerning distance from the sensor, and, in a subsequent phase, exploring temperature dependence.
- Homogeneity Measurement: Can the chosen sensors be adeptly utilized to measure the homogeneity of a Halbach ring-based B0 field within the stringent limit of less than 1000ppm? The desired outcome is a measurement of less than 50  $\mu\text{T}$  at 1000ppm, with a specific focus on determining the sensors' viability for noise measurements.

It is essential to emphasize that the intention is not to characterize the magnets; the sensors which might be used for characterisation are be analysed and evaluated.

This work prioritises the development of both hardware and software customised for sensor utilization and final testing. Physical properties and considerations take a secondary role in comparison to the overarching goal of refining the sensor-based methodologies.

## **1.5 Usecases**

The following section defines possible usecases that the future project need to cover. These usecases define the setup of the hard- and software. These illustrate practical situations to understand the functionality and added value of the implemented solution for the user.

The usecases were defined in the course of project planning and provide an overview of how the user interacts with the project and what functionalities can be expected. In the later accomplished evaluation process 5, the defined usecases are also used as a reference to demonstrate the implemented capabilities of the solution. This is essential for understanding the needs of the target group and designing the end result accordingly.

### **1. Ready to use hardware sensor designs**

A universal, easy-to-integrate Hall sensor design allows users to evaluate the framework quickly and cost-effectively. The pre-built hardware sensors provide an optimal solution for research, reducing development time and achieving repeatable measurement results. Once successfully evaluated, the Hall sensor design should be easily adaptable to other sensors without the need for major firmware changes.

### **2. Taking automatic measurements from sensors**

The purpose of the framework is to enable the automated acquisition of measurement data from various connected hardware sensors. The user should be able to configure various measurement series, which should then be carried out by the framework without further user interaction.

### **3. Open storage formats for data export**

The use of open storage formats for the export of data enables an interoperable data exchange environment. The implementation of standardized formats improves the portability and long-term availability of data. This encourages the exchange and further processing of measurement data in other software tools.

### **4. Ready to integrate data analysis functions**

Once it is possible to record and store measured values, it should be possible for the user to analyse and visualize this data using various algorithms. The focus here should be on extending the framework with user-created algorithms.

### 5. User programmable data processing pipelines

User-programmable data processing pipelines enable the flexible design of data processing sequences as pipeline by users. The framework should enable users to create their own pipelines with the previously defined data analysis functions.

## 1.6 Structure

This work is divided into six main chapters, which deal with the approach, implementation and evaluation. The techniques and concepts used are explained in detail. Specific examples provide an overview of the possible use of the developed solution by the user.

Chapter 2. **Unified Sensor** refers to the integration of different sensors into a standardised solution. This enables simple data acquisition and serves as a basic hardware system on which the subsequent data processing library can be applied.

Chapter 3. **Software Readout Framework** describes the implementation of the data readout framework. This includes an explanation of the various modules and specific application examples.

Chapter 4. **Usability Improvements** refers to additional activities to improve user-friendliness. This includes the optimisation of interfaces, interactions and processes to ensure intuitive and efficient use of the product. This also includes the documentation of code and the distribution of the source code as a package to users.

Chapter 5. **Usecase Evaluation** describes the application of the framework to the previously defined usecases and thus forms the basis for later evaluation.

Chapter 6. **Evaluation** outlines the evaluation process for permanent magnets using the developed framework. The research questions posed regarding the suitability of the sensors used for the characterisation of permanent magnets are examined.

Chapter 7. **Conclusion and Discussion** bringing together essential research components, it synthesizes study outcomes, discusses implications, and provides insights for future work. This section ensures closure and aids readers in grasping the broader context and significance of the research.

Finally, a comprehensive hardware and software framework needs to be established, which is capable of measuring diverse objects using various sensors. Additionally, remarks need to be provided regarding the suitability of the employed sensors for magnetic field measurements.

## 2 Unified Sensor

A defined main objective of this project is the development of a cost-effective magnetic field sensors interface that is universally expandable as well. The focus is on mapping different sensors and being compatible with different magnet types and shapes. This ensures a wide range of applications in different scenarios.

Another goal is reproducibility to ensure uniform results, which as a result reduces the susceptibility to errors. Easy communication with standard Personal Computer (PC) hardware, which offers a variety of common interface options, maximizes the user-friendliness.

The flexibility to support different sensors and magnets makes the system versatile and opens the possibility for use in different applications. A low-cost magnetic field sensors interface will therefore not only be economically attractive, but also facilitate the integration of magnetic field sensors in different contexts.

In addition, the low-cost sensor interface will serve as a development platform for the data evaluation MagneticReadoutProcessing (MRP) library and provide real measurement data from magnets. In addition, the interface firmware creates a basis for the development of a data protocol for exchanging measured values.

This makes it easy to integrate an own measuring devices into the MRP ecosystem at a later date. This is only possible with a minimal functional hardware and firmware setup and is developed for this purpose first.

### 2.1 Sensor Selection

The selection process for possible magnetic field sensors initially focussed on the most common and cost-effective ones, especially those that are already used in smartphones

and are therefore widely available.

A key aspect of this selection is the preference for sensors with digital interfaces to facilitate implementation in the circuit layout since these kind of sensors are easy to integrate compared to non-digital sensors, which require specific frameworks. The integration of integrated temperature sensors represents a significant enhancement that will later enable precise temperature compensation.

The use of analog sensors is purposefully avoided, though they are suitable for more precise measurements and extended measuring ranges. They were excluded because they require more carefully designed circuits and more complicated energy management.

In the context of the desired goal of developing a cost-efficient and universally expandable Hall sensor interface, the decision in favour of digital sensors seems appropriate.

Focussing on the digital Inter-Integrated Circuit (I2C) interface not only facilitates implementation, but also contributes to overall cost efficiency. At the same time, the integration of temperature sensors enables precise measurements under varying environmental conditions. This strategic choice forms the basis for a flexible, universally applicable Hall sensor interface that can be seamlessly integrated into various existing systems.

Table 2.1: Implemented digital magnetic field sensors

---

	TLV493D-A1B6	HMC5883L	MMC5603NJ	AS5510
Readout-Axis	3D	3D	3D	1D
Temperature-Sensor	yes	no	yes	no
Resolution [uT]	98	0.2	0.007	48
Range [mT]	±130.0	±0.8	±3	±50
Interface	I2C	I2C	I2C	I2C

---

The table 2.1 shows a selection of sensors for which hardware and software support

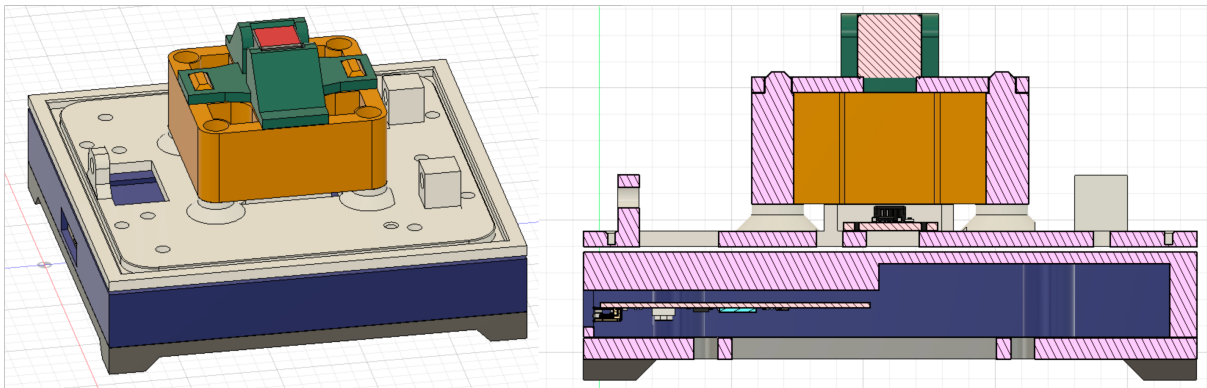


**Figure 2-1:** Mechanical components for the 1D sensor using 3D printed parts

has been implemented. The resolution of the selected sensors covers the expected range of values required by the various magnets to be tested.

In the Evaluation 6 chapter, basic characterisation methods are used to evaluate the sensors listed in 2.1 with regard to their sensitivity and other parameters. This is done at this point, as the components of the readout interface that enable interaction with the sensors are considered first.

## 2.2 Mechanical Structure

The mechanical design of a sensor is kept as simple as possible so that it can be replicated as easily as possible. The focus is on providing a stable foundation for the sensor Integrated Circuit (IC) and an exchangeable holder for different magnets.

The following figure 2-1, shows a sectional view of the CAD drawing of the 1D-Single sensor 2.5.1.

All parts are produced using the 3D printing additive manufacturing processes. The sensor circuit board is glued underneath the magnet holder. This is interchangeable, so different distances between sensor and magnet can be realised.

The exchangeable magnetic holder (shown in green) can be adapted to different magnets. It can be produced quickly due to the small amount of parts used. The two recesses lock the magnet holder with the inserted magnet over the sensor. The specified tolerances allow the magnet to be inserted into the holder with repeat accuracy and

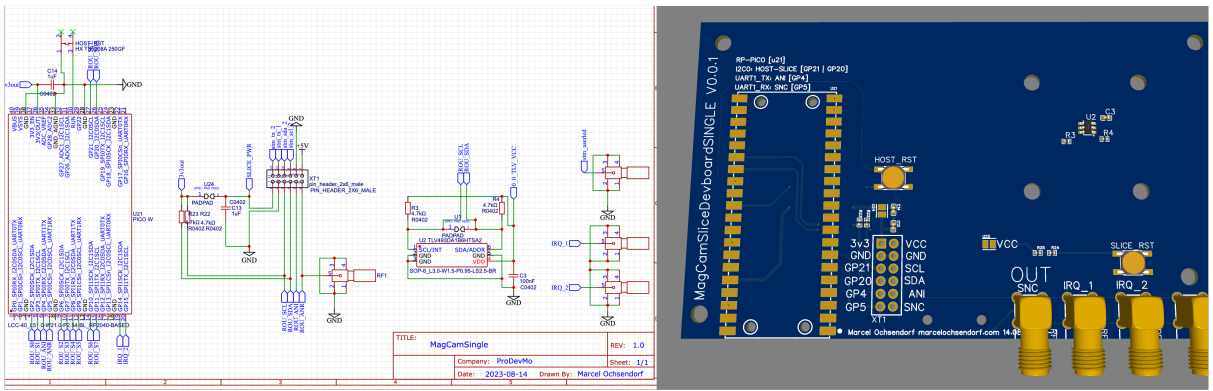


Figure 2-2: 1D sensor schematic and circuit board

without backlash. This is important if several magnets have to be measured, where the positioning over the sensor must always be the same.

## 2.3 Electrical Interface

The electronics consist of the magnetic field sensor and the electrical interface to connect it to a PC in the form of a microcontroller.

The focus is on utilising existing microcontroller development and evaluation boards, which already integrate all the components required for basic operation. This not only enabled a time-saving implementation, but also ensured a cost-efficient realisation.

All the necessary components and their circuitry are recorded on a Printed Circuit Board (PCB) 2-2 and subsequently manufactured. In addition, footprints are provided for various sensor IC packages. By placing mounting holes on the PCB, it is possible to attach various mechanical mounts on top of the sensor ICs.

Special attention is paid to the provision of an accessible SYNC-General Purpose Input/Output (GPIO) connector. This enables subsequent multi-sensor synchronization and also offers options for later extensions. This functionality opens up the possibility of synchronising data from different sensors to achieve precise and coherent measurement results. Overall, this integrated approach represents an effective solution for the flexible evaluation of sensors and helps to optimise the development process.

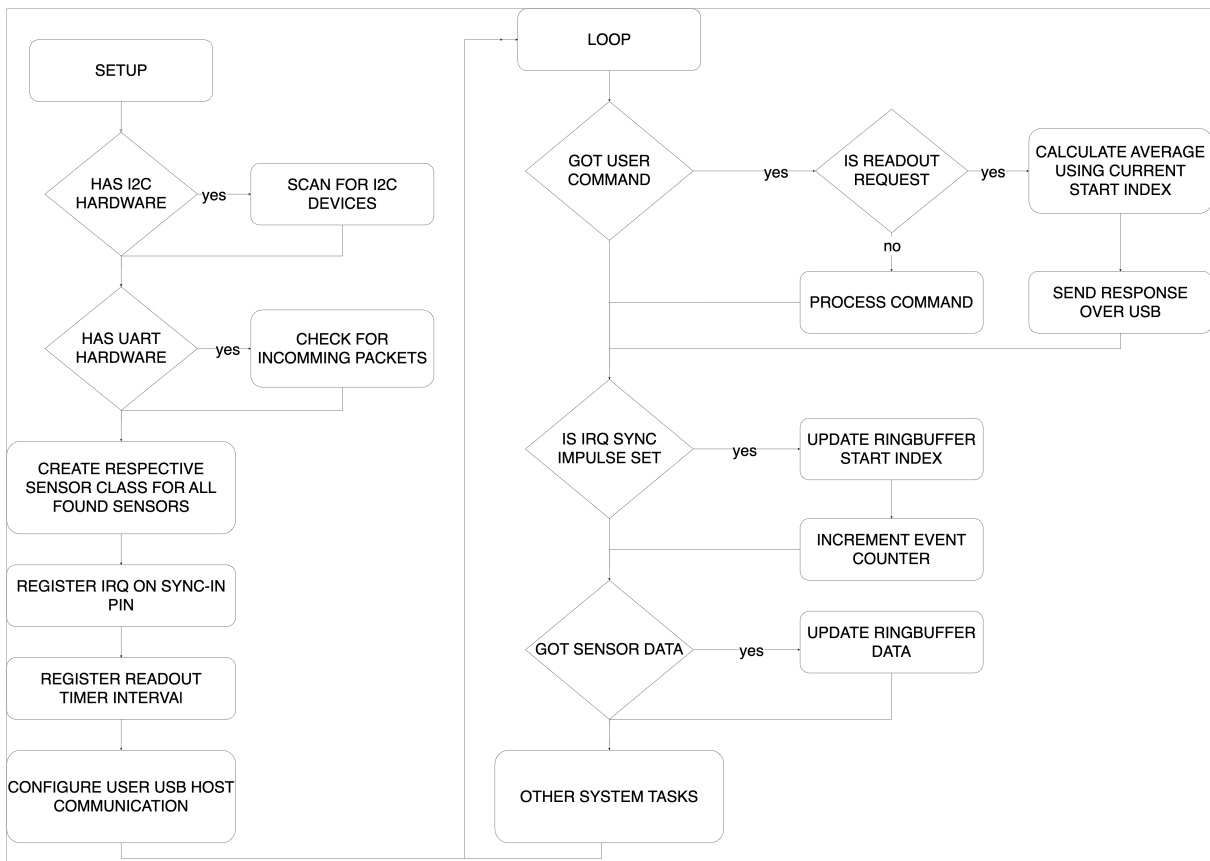


Figure 2-3: Unified sensor firmware simplified program structure

## 2.4 Firmware

The microcontroller firmware is software that is executed on a microcontroller in an embedded system. It controls the hardware and enables the execution of predefined functions. The firmware is used to process input data, control output devices and performs specific tasks according to the program code.

It handles communication with sensors, actuators and other peripheral devices, processing data and making decisions. Firmware is critical to the functioning of devices.

The firmware is responsible for detecting the possible connected sensors 2.1 and query measurements. This measured data can be forwarded to a host PC via a user interface and can then be further processed there.

An important component is that as many common sensors as possible can be easily connected without having to adapt the firmware. This modularity is implemented using abstract class design. These are initiated according to the sensors found at startup. If new hardware is to be integrated, only the required functions 2.1 need to be

implemented.

```
1 #ifndef __CustomSensor_h__
2 #define __CustomSensor_h__
3 // register your custom sensor in implemented_sensors.h also
4 class CustomSensor: public baseSensor
5 {
6 public:
7     CustomSensor();
8     ~CustomSensor();
9     // implement depending sensor communication interface
10    bool begin(TwoWire& _wire_instance); // I2C
11    bool begin(HardwareSerial& _serial_instance); // UART
12    bool begin(Pin& _pin_instance); // ANALOG or DIGITAL PIN like onewire
13    // FUNCTIONS USED BY READOUT LOGIC
14    bool is_valid() override;
15    String capabilities() override;
16    String get_sensor_name() override;
17    bool query_sensor() override;
18    sensor_result get_result() override;
19 };
20 #endif
```

Listing 2.1: CustomSensor-Class for adding new sensor hardware support

The flow chart 2-3 shows the start process and the subsequent main loop for processing the user commands and sensor results. When the microcontroller is started, the software checks whether known sensors are connected to I2C or Universal Asynchronous Receiver / Transmitter (UART) interfaces.

If any are found (using a dedicated Lookup Table (LUT) with sensor address translation information), the appropriate class instances are created and these can later be used to read out measurement results.

The next initialisation system is dedicated for multi-sensor synchronisation 2.4.2. The last step in the setup is to configure communication with the host or connected PC. All implemented microcontroller platforms used (*Raspberry Pi Pico, STM32F4*) have a Universal Serial Bus (USB) slave port.

The used usb descriptor is a USB Communication Device Class (CDC). This is used to emulate a virtual *RS232* communication port using a USB port on a PC and usually no additional driver is needed on modern host systems.

```
help
=====
> help                      shows this message
> version                   prints version information
> id                        sensor serial number for identification purposes
> sysstate                  returns current system state machine state
> opmode                     returns 1 if in single mode
> sensorcnt                returns found sensorcount
> readsensor x <0-senorcount> returns the readout result for a given sensor index for X axis
> readsensor y <0-senorcount> returns the readout result for a given sensor index for Y axis
> readsensor z <0-senorcount> returns the readout result for a given sensor index for Z axis
> readsensor b <0-senorcount> returns the readout result for a given sensor index for B axis
> temp                       returns the system temperature
> anc <base_id>             perform a autonumbering sequence manually
> ancid                      returns the current set autonumbering base id (-1 in singlemode)
> reset                      performs reset of the system
> info                        logs sensor capabilities
> commands                   lists sensor implemented commamnds which can be used by hal
=====
```

**Figure 2-4: Sensors CLI**

After execution of the setup routine is completed, the system switches to an infinite loop, which processes several possible actions. One task is, to react to user commands which can be sent to the system by the user via the integrated Command Line Interface (CLI). All sensors are read out via a timer interval set in the setup procedure and their values are stored in a ring buffer. Ring buffer offers efficient data management in limited memory. Its cyclic structure enables continuous overwriting of older data, saves memory space and facilitates seamless processing of real-time data.

Ring buffers are well suited for applications with variable data rates and minimise the need for complex memory management. The buffer can be read out by command and the result of the measurement is sent to the host. Each sensor measurement result is transmitted from the buffer to the host together with a time stamp and a sequential number. This ensures that in a multi-sensor setup with several sensors. The measurements are synchronized 2.4.2 in time and are not out of sequence or drift.

#### **2.4.1 Communication Interface**

Each sensor that is loaded with the firmware, registers on to the host PC as a serial interface. There are several ways for the user to interact with the sensor:

- Use with MRP 3-library
- Stand-alone mode via sending commands using built-in CLI

```
readsensor b 0
3279.99
```

Figure 2-5: Query sensors b value using CLI

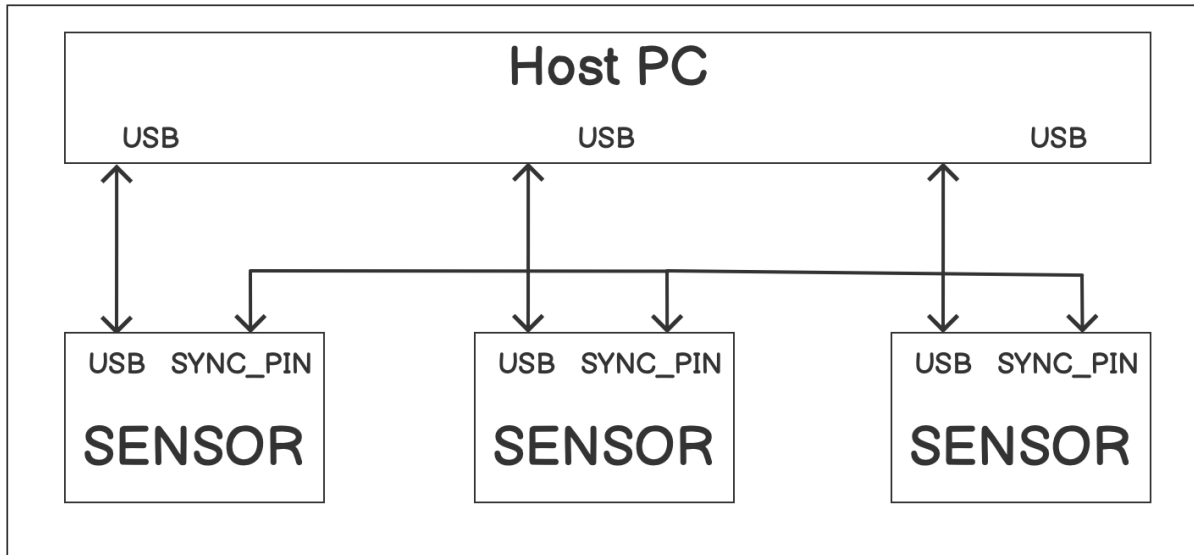


Figure 2-6: Multi sensor synchronisation wiring example

The CLI mode is a simple text-based interface with which it is possible to read out current measured values, obtain debug information and set operating parameters. This allows to quickly determine whether the hardware is working properly after installation. The CLI behaves like terminal programmes, displaying a detailed command reference 2-4 to the user after connecting. The current measured value can be output using the *readout* command 2-5.

The other option is to use the MRP 3-library. The serial interface is also used here. However, after a connection attempt by the Hardware Abstraction Layer (HAL) 3.4.2 module of the MRP 3-library, the system switches to binary mode, which is initiated using the *sbm* command. The same commands are available as for CLI-based communication, but in a binary format.

#### 2.4.2 Sensor Syncronisation Interface

One problem with the use of several sensors on one readout host PC is that the measurements may drift over time. On the one hand, USB latencies can occur. This can occur due to various factors, including device drivers, data transfer speed and system

resources. High-quality USB devices and modern drivers often minimise latencies. Nevertheless, complex data processing tasks and overloaded USB ports can lead to delays.

Table 2.2: Measured sensor readout to processing using host software

Data- Points	Run [ms]	Average Sensor communication time per reading [ms]	Communication jitter time [ms]	Comment
1	9453	1.44	0	
1	9864	1.5	0	
10	12984	1.22	0.9	
10	12673	1.13	1.1	
10	43264	2.19	8.2	96% system load

The table shows 2.2 shows various jitter measurements. These were performed on a *Raspberry Pi 4 4GB-Single Board Computer* (SBC) together with an *1D: Single Sensor 2.5.1* and the following software settings:

- *Raspberry Pi OS Lite* - Operating System (OS) *Debian bookworm x64*,
- MRP 3-library - Version *1.4.1*
- Unified Sensor 2-firmware - Version *1.0.1*

It can be seen that a jitter time of up to an additional *1ms* is added between the triggering of the measurements by the host system and the receipt of the command by the sensor hardware. If the host system is still under load, this value increases many times over. This means that synchronising several sensors via the USB connection alone is not sufficient.

The other issue is sending the trigger signal from the readout software 3. Here too, unpredictable latencies can occur, depending on which other tasks are also executed

on this port.

In order to enable the most stable possible synchronisation between several sensors, an option has already been created to establish an electrical connection between sensors. This is used together with the firmware to synchronise the readout intervals. The schematic 2-6 shows how several sensors must be wired together in order to implement this form of synchronisation.

Once the hardware has been prepared, the task of the firmware of the various sensors is to find a common synchronisation clock. To do this, the function *register irq on sync pin* is overwritten. To set one *primary* and several *secondary* sensors, each sensor waits for an initial pulse on the SYNC-GPIO 2-7. Each sensor starts a random timer beforehand, which sends a pulse on the sync line. All others receive this and switch to *secondary* mode and synchronise the measurements based on each sync pulse received.

Since the presumed *primary* sensor cannot register its own sync pulse (because the pin is switched to output), there is a timeout branch condition *got pulse within 1000ms* and this becomes the *primary* sensor. This means that in a chain of sensors there is exactly one *primary* and many *secondary* sensors.

In single-sensor operation, this automatically jumps to *primary* sensor operation through the *got impulse within 1000ms* branch result. The synchronisation status can be queried via the user interface 2.4.1 using the *opmode* 2-8 command. An important aspect of the implementation here is that there is no numbering or sequence of the individual sensors.

This means that for the subsequent readout of the measurements, it is only important that they are taken at the same interval across all sensors. The sensor differentiation takes place later in the MRP 3-library by using the sensor Universal Unique Identifier (UUID).

## 2.5 Example Sensors

Two functional sensor platforms 2.3 are built in order to create a solid test platform for later tests and for the development of the MRP 3-library with the previously developed sensor concepts.

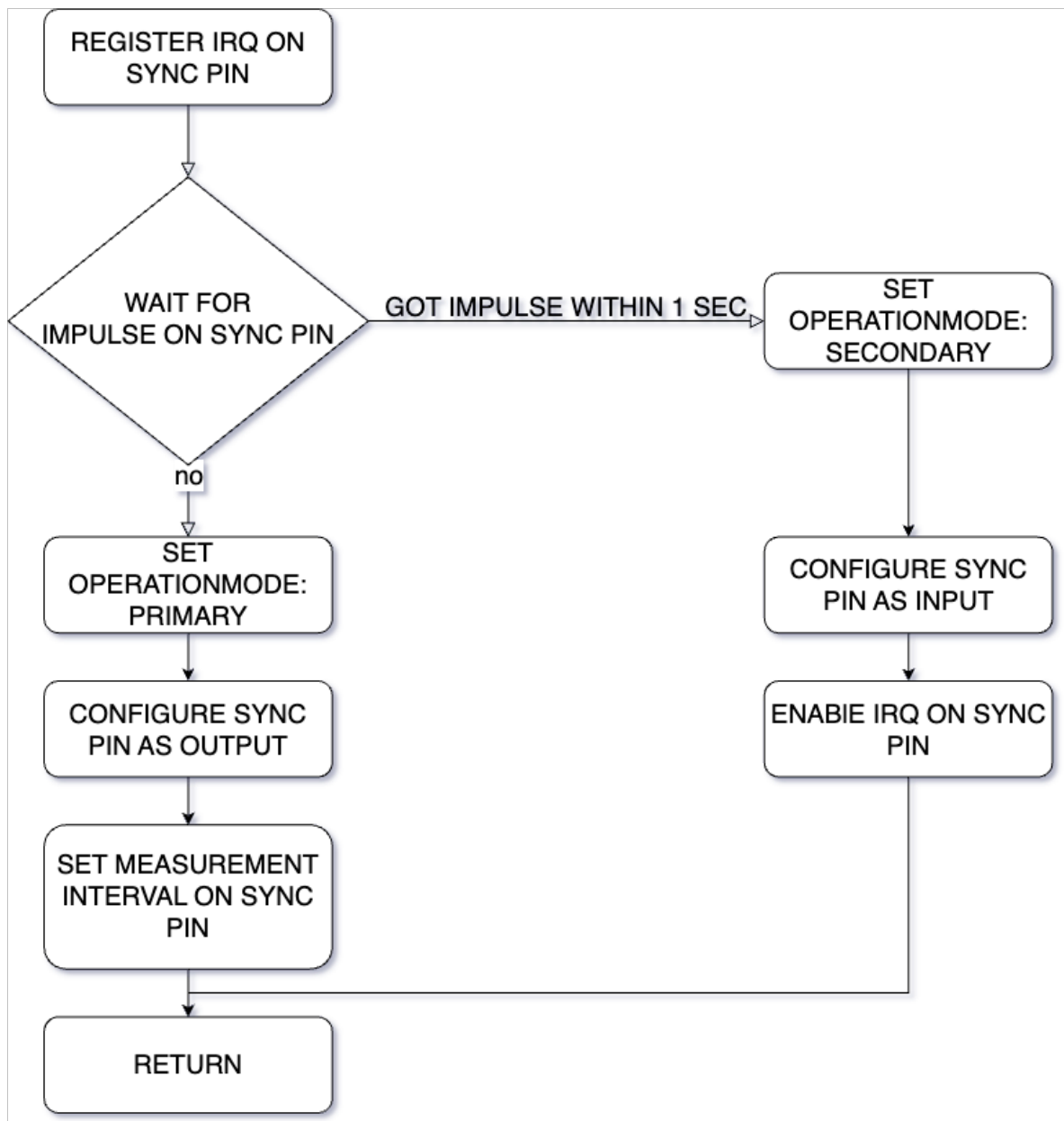


**Figure 2-7:** Unified sensor firmware multi sensor synchronisation procedure

```

opmode
SECONDARY (got sync after 823ms)
  
```

**Figure 2-8:** Query opmode using CLI

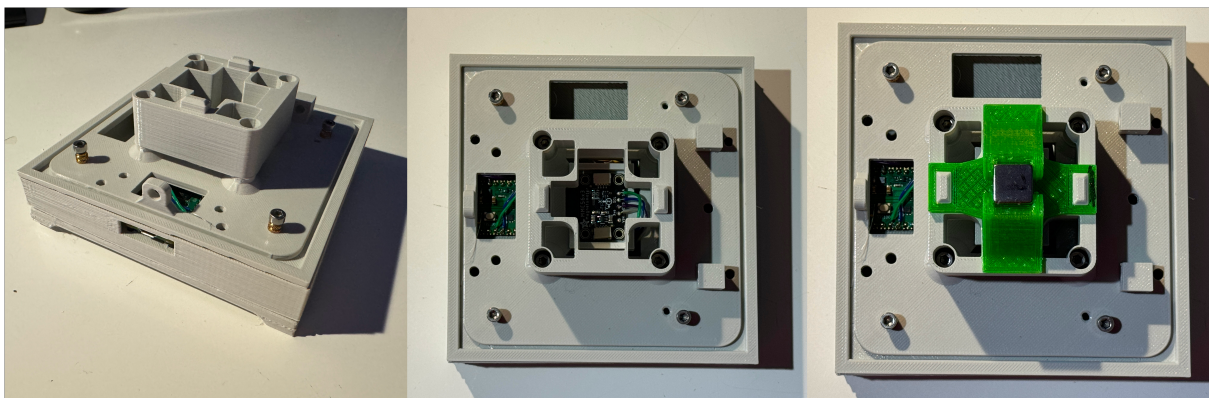


**Figure 2-9:** 1D sensor construction with universal magnet mount

**Table 2.3:** Build sensors with different capabilities

	1D2.5.1	1D: dual sensor	3D: Fullsphere??
Maximal magnet size	Cubic 30x30x30	Cubic 30x30x30	Cubic 20x20x20
Sensor type	MMC5603NJ	TLV493D	TLV493D
Sensor count	1	2	1
Scanmode	static (1 point)	static (2 points)	dynamic (fullsphere)

These cover all the required functions described in the usecases 1.5. The most important difference, apart from the sensor used, is the *scan mode*. In this context, this describes whether the sensor can measure a *static* fixed point on the magnet or if the sensor can move *dynamically* around the magnet using a controllable manipulator.

In the following, the hardware structure of a *static* and *dynamic* sensor is described. For the *static* sensor, only the *1D* variant is shown, as this does not differ significantly from the structure of the *1D: dual sensor*, except it uses two *TLV493D* sensors, mounted above and on top of the magnet.

### 2.5.1 1D: Single Sensor

The 1D sensor **2-9** is the simplest possible sensor that is compatible with the Unified Sensor firmware 2.4 platform.

The electrical level here is based on a *Raspberry-Pi Pico* together with the *MMC5603NJ* magnetic sensor. The mechanical setup consists of four 3D printed components, which are fixed together with nylon screws to minimise possible influences on the measurement.

Since the *MMC5603NJ* only has limited measurement range of total  $6\mu T$ , even small coin sized neodymium magnets already saturates the sensor. It is possible to mount 3D printed spacers over the sensor to increase the distance between the magnet and the sensor and thus also measure these magnets.

The designed magnet holder can be adapted for different magnet shapes and can be placed on the spacer without backlash in order to be able to perform a repeatable measurement without introducing measurement irregularities by mechanically changing the magnet.

### 2.5.2 3D: Full Sphere

The 3D full sphere sensor **2-10** offers the possibility to create a 3D map of the inserted magnet.

The graphic **2-11** shows the visualisation of such a scan in the form of a spherical 3D map. On the sphere is the magnetic field strength, which is detected by the sensor at the position. The transition from a fully positive field strength (red) to a negative field strength (blue) is clearly recognisable and corresponds to the orientation of the magnet in the holder.

The magnet sensor is mounted on a movable arm, which can move 180 degrees around the magnet on one axis. In order to be able to map the full sphere, the magnet is mounted on a turntable. This permits the manipulator to move a polar coordinate system.

As the magnets in the motors, as with the screws used in the 1D sensor, can influence

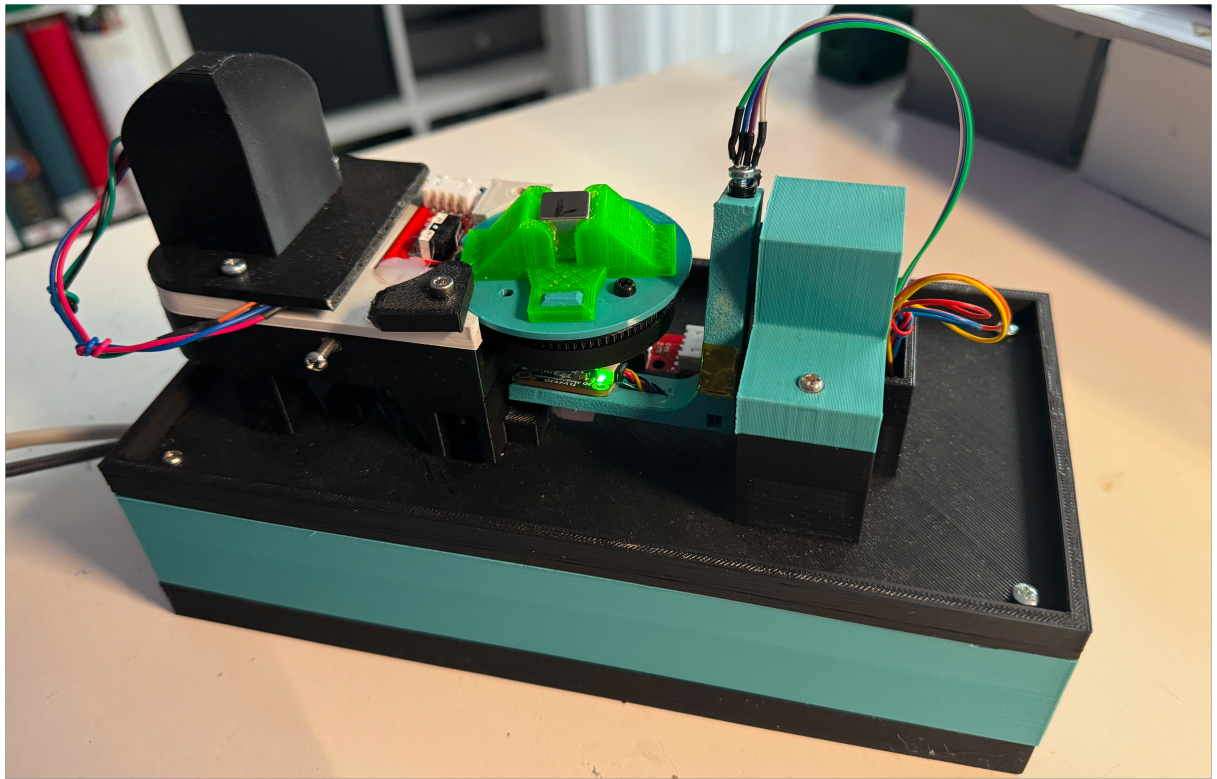


**Figure 2-10:** Full-Sphere sensor implementation using two Nema17 stepper motors in a polar coordinate system

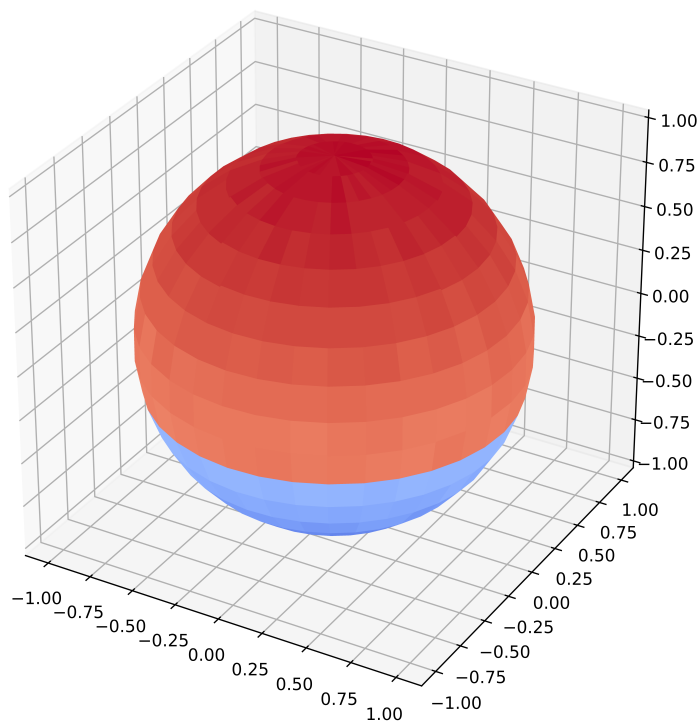


**Figure 2-11:** 3D plot of an N45 12x12x12 magnet using the 3D fullsphere sensor

the measurements of the magnetic field sensor, the distance between these components and the sensor or magnets is increased. The turntable and its drive motor are connected to each other via a belt.

On the electrical side, consists of a *SKR-Pico* stepper motor controller on the one hand side and a *TLV493D* magnetic field sensor on the other hand side. This is chosen because of its larger measuring range and can therefore be used more universally without having to change the sensor of the arm.

### 2.5.3 Integration of an Industry-Teslameter

As the sensors shown so far relate exclusively to self-built, low-cost hardware, the following section shows how existing hardware can be integrated into the system. A temperature-compensated *Voltcraft GM-70* telsameter 2-12 is used, which has a measuring range of  $0T$  to  $3T$  with a resolution of  $0.1mT$ . It offers an *RS232* interface with a documented protocol for connection to a PC.

This connectivity makes it possible to make the device compatible with the unified sensor ecosystem using a separate interface software [21] executable on the host PC. However, it does not offer the range of functions that the unified sensor firmware offers.

Another option is a custom interface board between the meter and the PC. This is a good option as many modern PCs or SBCs no longer offer an physical *RS232* interface. As with the other sensors, this interface consists of a *Raspberry-Pi Pico* with an additional level shifter.

The teslameter is connected to the microcontroller using two free GPIOs in UART mode. The firmware is adapted using a separate build configuration. In order to be able to read and correctly interpret the data from the microcontroller, the serial protocol of the sensor is implemented in a customised version of the *CustomSensor* class 2.1.

This software or hardware integration can be carried out on any other measuring device with a suitable communication interface and a known protocol thanks to the modular design.

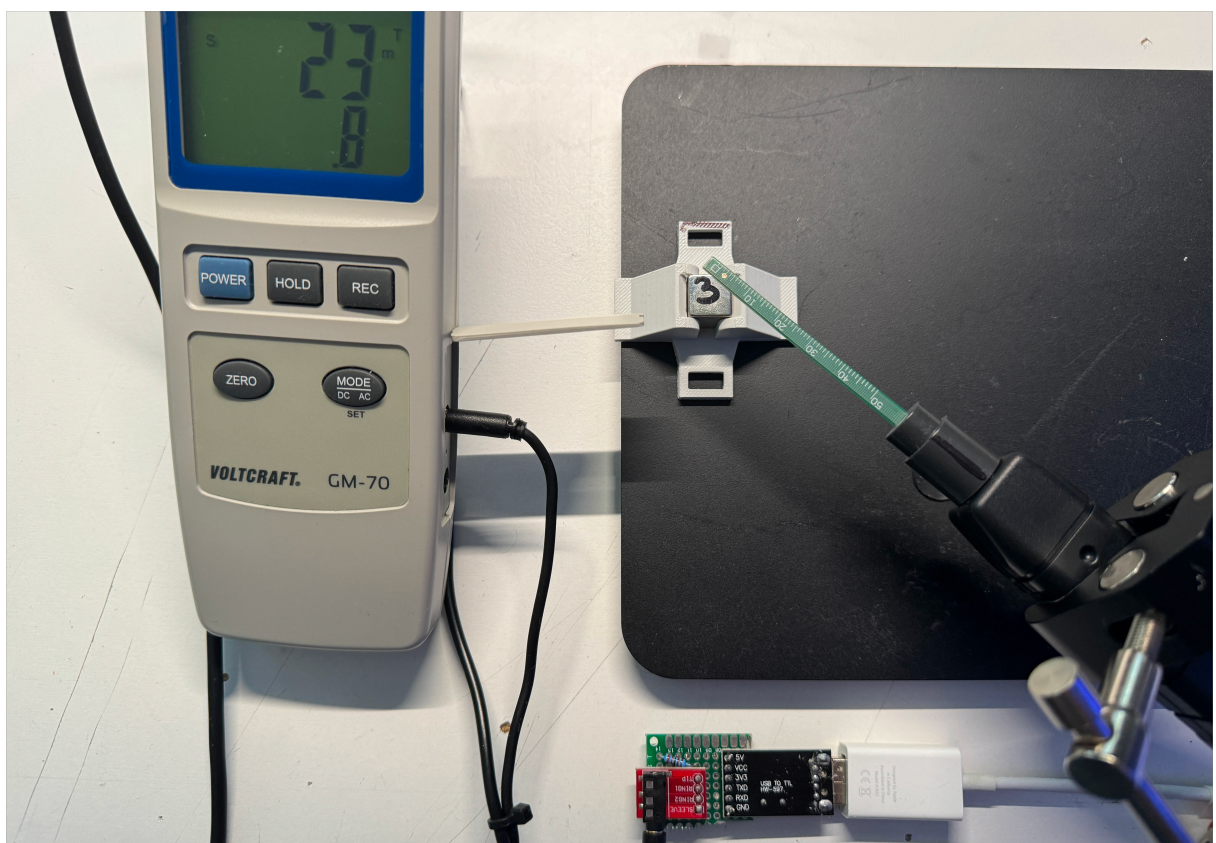


Figure 2-12: Voltcraft GM70 teslameter with custom PC interface board

# 3 Software Readout Framework

The software readout framework is the central software component that is developed as part of this work. This software framework is intended to provide a user-oriented data acquisition and analysis environment. For this purpose, typical individual steps that occur in relation to these tasks are implemented:

- Data acquisition - from hardware sensors or other data sources
- Storage - export of data in various open formats 3.2.2
- Analysis - algorithms to analyse different data sets 3.2.3

All these possible task parts are divided into different blocks and users are given the possibility of adding their own functionalities.

As the following, this concept is referred to as *user interaction points* 3.1 and is explained in the following chapter.

## 3.1 User Interaction Points

User interaction points represent the core concept of the developed library and are intended to provide user-friendliness on the one hand and the rapid development of own analysis and optimisation algorithms on the other.

For this purpose, the library is divided into individual modules, which are shown in the graphic 3-1. In combination, these represent a typical measurement-analysis-evaluation workflow of data. For this purpose, a module system with standardised functional patterns and data types is developed and packed together in an extendable Python library.

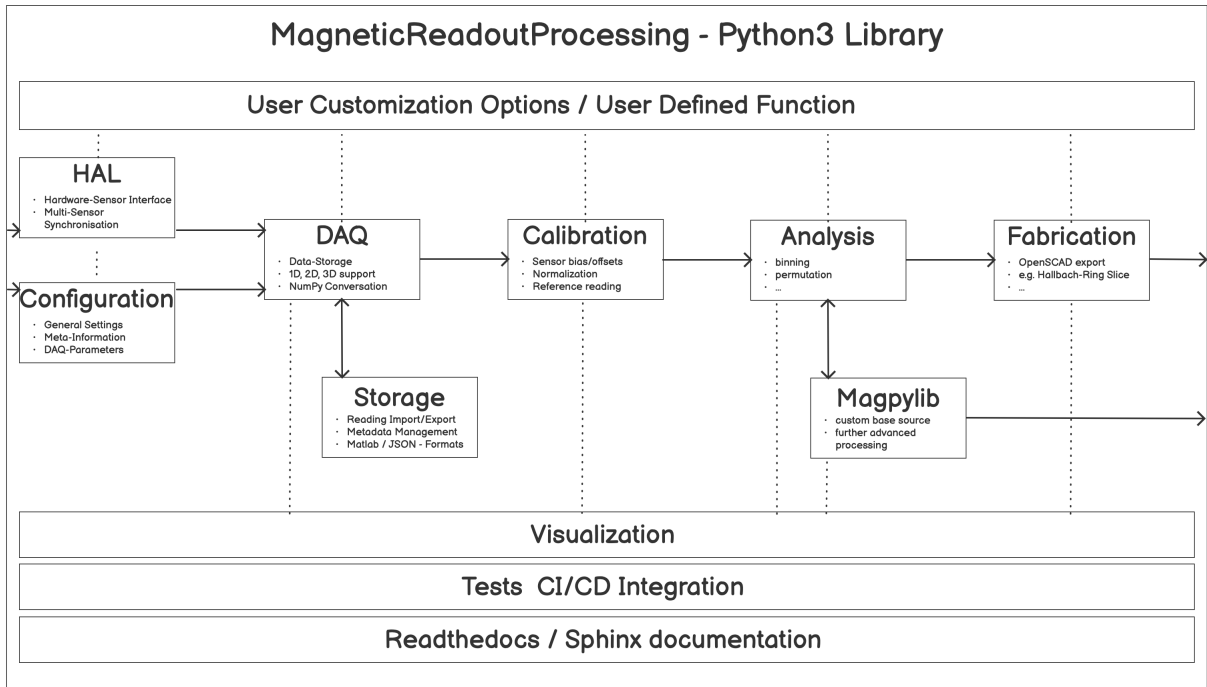


**Figure 3-1:** MRP library module high level overview

According to this concept, the user should be able to replace individual components from this chain with their own modules without having to worry about implementing other of these to make the project work.

#### 3.1.1 User Interaction Points Example

The following example shows the advantages of using the *User interaction points*:

A project called *HalbachOptimisation* [23] implements a data analysis step and optimizes a magnetic field that is as homogeneous as possible within a circular section using given mechanical dimensions as input parameters of the magnets used. For this purpose, a mutation of the magnet positions and rotations is performed. The result is a list of positions for each magnet.

The *HalbachMRIDesigner* [2] opensource project, can generate basic CAD drawings for MRI magnets in a Halbach configuration. To do this, the number of magnets and additional parameters for the properties of the CAD model to be created are passed to the function provided as input parameters using a JavaScript Object Notation (JSON) file. The result is an *OpenSCAD* [18] based 3D model of the magnet holder.

As a result, there are two projects which are both suitable for the task of optimizing and

creating Halbach magnets for MRI applications. The data structures are not compatible with each other. However, they are executed manually one after the other to obtain a final result with manual data conversation.

The library created is intended to solve one problem by providing standardized and flexible data structures for use with this form of magnetic field data. By separating the processing pipeline into defined sub-steps, it should be possible to make individual modules and as a result functionalities interchangeable by the user.

The implementation of the same functionalities looks as follows after using the library:

#### 1. Create a static set of magnets

The input parameters of the *HalbachOptimisation* [23] project are on the one hand the mechanical dimensions and the number of magnets to be used. We assume ideal magnets here. However, it should also be possible to import field data in a more measured form later on. Using the DataAquisition sub-step, it is possible to generate any number of ideal magnets.

#### 2. Add custom analysis processing step

Next, the user creates his own analysis step in order to be able to call up its functions. In the case of the *HalbachOptimisation* [23] project, the function signature of the start function must be changed. This receives the result of the previous step, in this case the generated magnet data. By optionally setting meta data in the universal library data type, constants can be replaced in the analysis function and made dynamically configurable. The return result also corresponds to this data type so that subsequent steps are compatible and contains the magnet data with modified position and rotation data.

#### 3. Generate fabrication data

The last step is to call up the *HalbachMRIDesigner* [2] project, which creates the CAD model of the magnet holder. The data can also be exported as files here. To make the project compatible, the function signatures are also adapted here. In this case, more changes are required, as the configuration file is loaded from the file system. This logic must be removed in order to use the added meta data in the input parameter instead.

After these customisation steps, it is possible to execute both projects one after the other

and all required configuration parameters are contained in the data structure looped through the individual steps as meta data. This also maps the functionality of a project file, which can be executed or passed on repeatedly.

This also fulfils the goal of making individual user-created algorithms interchangeable. If the user now wishes to use a different CAD algorithm instead of the *HalbachMRIDesigner* [2], the other steps can simply be preserved and only the new step needs to be implemented.

## 3.2 Modules

In order to realise the concept of user interaction points, the library is divided into different modules. These modules can be divided into two main categories:

- Core - All modules related to measurement data management
- Extensions - Contains modules for visualisations, hardware sensor access

In each of these categories there are then several sub-categories divided into User Interaction Points. An overview of these is given in the subchapters as the following. There are also introductory examples which provide an overview of the basic functions in the *Examples 3.4* section, as well as further examples in the online documentation [5].

### 3.2.1 Core Modules

The included core modules are essential for using the library. Basic data types are implemented, as well as functions for import and export. In addition, there are other support scripts that are required internally.

The following modules are implemented in detail:

- *MRPReading* - storage of measured values
- *MRPMeasurementConfig* - storage of the measurement parameters
- *MRPMagnetTypes* - various physical constants for basic magnet types

The *MRPReading* module performs a essential role in streamlining the centralized management of measurement data. It serves as a storage provider for various measurements, offering functionalities that facilitate the creation and addition of data records. To customise and add meta-data, users have the flexibility to configure parameters through the dedicated *MRPMeasurementConfig* module into an *MRPReading* instance.

Within the realm of measurement data, a diverse range of data points can be seamlessly incorporated. The process is initiated by employing specialized functions designed for the creation and addition of data records.

To configure parameters, ensuring a tailored approach to the entire measurement process, these parameters act as a essential bridge between user preferences and the robust capabilities of the *MRPReading* module.

The system is also designed to be compatible with *Extension Modules 3.2.3*, allowing the generation of measurement data through various modules. This extensibility enhances the versatility of the system, accommodating diverse measurement scenarios and expanding its utility across different domains.

To enhance the accessibility and interpretability of the recorded data, a dedicated module, *MRPMagnetTypes*, comes into play. This module is specifically designed for the storage of physical parameters pertaining to the magnets targeted for measurement.

By centralizing this information, users can streamline the subsequent phases of evaluation and analysis, simplifying the overall process and ensuring a more efficient and insightful exploration of the collected data.

At the end of processing, the collected and modified data are typically exported; various functions are provided for this purpose. This process is described in the following subchapter.

#### 3.2.2 Storage and Datamanagement

An important aspect is data import and export. On the one hand, this allows the library to reuse and archive the measurements. On the other hand, the focus during development is that it is also possible to use the data in other programs.

For this purpose, an open, documented export format must be selected. Ideally, this

should be human-readable and viewable with a simple text editor. This eliminates all binary-based formats such as the Python pickle built into Python.

Taking these points into account, the JSON format is chosen. This is human and machine readable and there is a compatible parser for almost every programming language.

The following code snippet 3.1 shows the JSON structure which is generated when a measurement that using the library is exported. It can be seen that by using the JSON format, all measurement points and metadata are available in readable plain text.

This means that they can also be read out in other programs. Using serialization, the *MRPReading* class inherited from Python-*Object* class is serialized via an dictionary conversion step. This JSON string can then be processed directly or written to the file system as a file.

```
1 {
2     "time_start": "Wed Sep 20 08:50:13 2023",
3     "time_end": "Wed Sep 20 08:54:13 2023",
4     "additional_data": {
5         "sensor_device_path": "/dev/ttyUnifiedSensorSingle",
6         "sensor_name": "Unified Sensor Single Sensor",
7         "sensor_id": "386731533439",
8         "sensor_capabilities": ["static", "axis_b", "axis_x", "axis_y", "axis_z", "axis_temp", "axis_stimestamp"],
9         "configname": "calibrationtemp30.yaml",
10        "runner": "cli"
11    },
12    "data": [
13        {
14            "value": 0.135,
15            "is_valid": true,
16            "id": 0,
17            "temperature": 34.32
18        },
19        "measurement_config": {
20            "id": "525771256544952",
21            "sensor_distance_radius": 40.0,
22            "magnet_type": 0
23        },
24        "name": "calibrationtemp30",
25    }
}
```

Listing 3.1: JSON export structure of an MRPReading based measurement

The exported example 3.1 contains the following different object keys, which contain the

following information:

- *additional\_data* - Additional user-defined metadata
- *data* - Datapoint storage consists of measured value, UUID and temperature, among other parameters
- *measurement\_config* - Information about the sensor used for measurement

In addition, further custom objects can be inserted into the JSON using the functions provided.

Since there are popular data processing frameworks such as *Numpy* [16], or the program for mathematical calculations, *MATLAB* are often used, the library also supports export formats for these systems.

The different formats can be triggered by the user by calling up the corresponding *MRPReading* class functions:

- `*.dump()` - JSON
- `.to_numpy_matrix()` - *Numpy*-Array of *data* object with different options
- `.dump_savemat()` - *MATLAB* mat-file with measurement values and temperatures

Currently, data re-import of an exported measurement is only supported via the JSON format, as an export using the other options (*Numpy*, *MATLAB*) loses data during the export procedure.

#### 3.2.3 Extension Modules

The extension modules build on the core modules and offer the user additional basic functionalities. These include functions for data acquisition, visualisation and analysis.

##### Sensor Interface

Another collection of optional modules provided by the library is the connection of external hardware sensors. All compatible sensors that are compatible with the firmware developed in the *Unified Sensor 2* chapter are supported here. The library provides the following sensor HAL modules for this purpose:

- *MRPHal* - Firmware protocol implementation
- *MRPHalLocal* - USB sensor interface
- *MRPHalRemote* - Remote sensor interface

These provide functions to communicate with a connected hardware sensor and send commands to it. To generate these and convert the received measurement data into the appropriate format for the core modules, there is a suitable module for each sensor type:

- *MRPReadingSourceStatic* - for 1D and 2D sensors such as *1D: Single Sensor 2.5.1*
- *MRPReadingSourceFullsphere* - for 3D sensors such as *3D: Fullsphere ??*

The decision which of these modules to use is made automatically depending on the connected hardware. For this purpose, a static function *createReadingSourceInstance* is implemented in the base class *MRPReadingSource*, which automatically creates the appropriate instance based on the sensor capabilities.

## Visualisation

In order to give the user the possibility to display the recorded data visually, two modules were created, which can graphically prepare *MRPReading* instances:

- *MRPVisualization* - different table and graph based plots
- *MRPPolarVisualization* - fullsphere map plots

On the one hand, it is possible with the *MRPVisualization* module to display measurement data as a table or plot (e.g. stream, line, point). This makes it possible, for example, to visually identify outliers or trends in the measurement data. These can also be saved as an image file. The module is compatible with all measurement data.

In contrast to the *MRPPolarVisualization* module, this provides functions to create 2D map plots a polar coordinate system. This requires measurement data with additionally set spatial coordinates. These can be generated automatically with the *3D: Fullsphere ??* sensor, or the user must provide the spatial information from another source.

## Analysis

Data analysis offers the user the greatest flexibility to implement their own modules. For this reason *MRPAnalysis* contains functions for calculating the following data analyses, which are compatible with class instances of *MRPReading*:

- *std\_deviation* - Standard deviation
- *mean* - Mean value
- *variance* - Variance
- *CoG* - Centre of gravity
- *binning* - Distribution of a sample by means of a histogram
- *k-nearest* - K-nearest neighbours

In addition, the export function *.to\_numpy\_matrix* enables further processing of the data in the *Numpy* [16] framework, in which many other standard analysis functions are implemented.

## 3.3 Multi Sensor Setup

At the current described scenarios, it is only possible to detect and use sensors that are directly connected to the host PC. It has the disadvantage that there must always be a physical connection. This can make it difficult to install multiple sensors in measurement setups where space or cable routing options are limited.

Multiple sensor can be connected to any PC which is available on the network. This can be a SBC (e.g. a Raspberry Pi). The small footprint and low power consumption make it a good choice. It can also be used in a temperature chamber.

The *MRPProxy 3-2* module has been developed to allow forwarding and interaction with several sensors over a network connection using a Representational State Transfer (REST) interface.

The approach of implementing this via a REST interface also offers the advantage that several measurements or experiments can be recorded at the same time with one remote sensor setup.

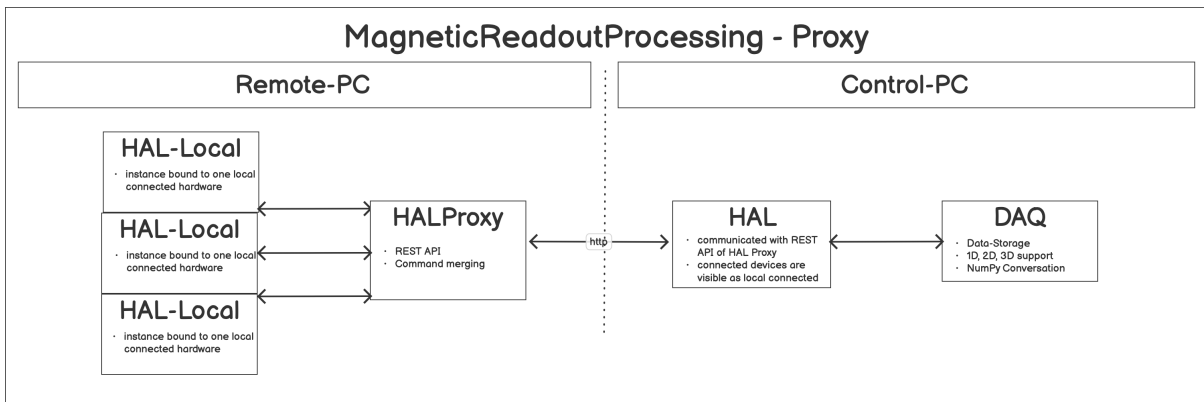


Figure 3-2: MRPlib Proxy Module

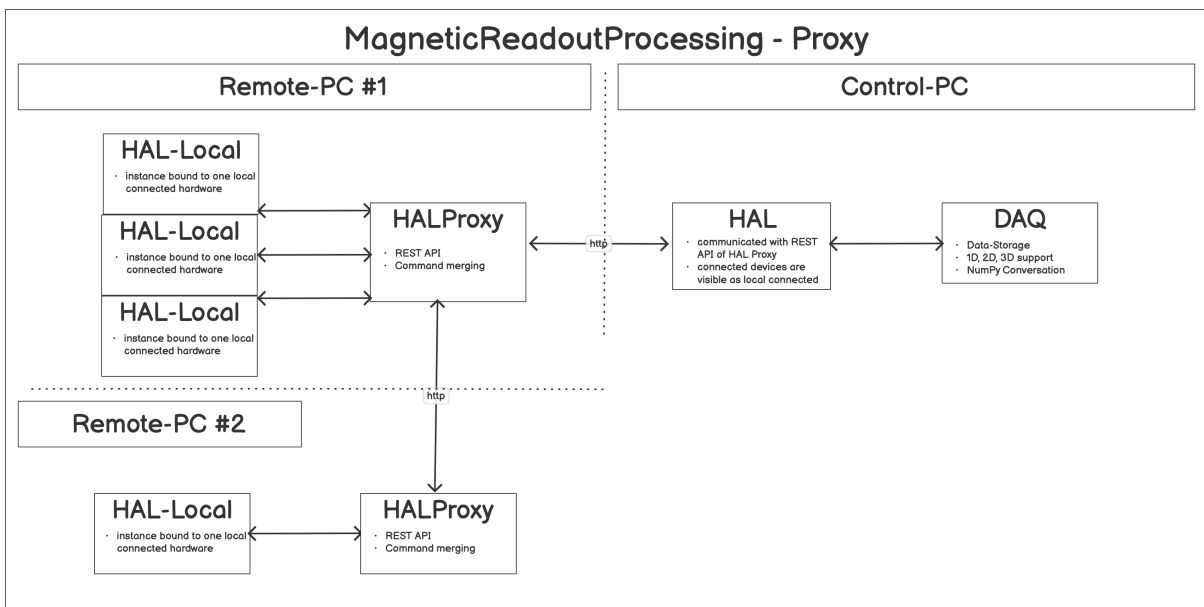


Figure 3-3: Example MRP proxy module usage, using two remote PCs

Another application example is when sensors are physically separated or there are long distances between them. By connecting several sensors via the proxy module, it is possible to link several instances and all sensors available in the network are available to the *control* PC.

The figure 3-3 shows the modified *multi-proxy - multi-sensor* topology. Here, both proxy instances do not communicate directly with the *control* PC, but the proxy instance *remote PC #2* can access the proxy running on *remote PC #1*.

The *control* PC only communicates with the *remote PC #1*, but can access all sensors in this chain.

### 3.3.1 Network-Proxy

The figure 3-2 shows the separation of the various HAL instances, which communicate with the physically connected sensors on the *remote* PC and the *control* PC side, which communicates with the remote side via the network. For the user, nothing changes in the procedure for setting up a measurement. The *MRPProxy* CLI application must always be started 3.2 on the PC with connected hardware sensors attached.

```
1 # START PROXY INSTNACE WITH TWO LOCALLY CONNECTED SENSORS
2 $ python3 mrpproxy.py proxy launch /dev/ttySENSOR_A /dev/ttySENSOR_B #
   add another proxy instance http://proxyinstance_2.local for multi-
   sensor, multi-proxy chain
3 Proxy started. http://remote_pc.local:5556/
4 PRECHECK: SENSOR_HAL: 1337 # SENSOR A FOUND
5 PRECHECK: SENSOR_HAL: 4242 # SENSOR B FOUND
6 Terminate Proxy instance [y/N] [n]:
```

Listing 3.2: MRPproxy usage to enable local sensor usage over network

After the proxy instance has been successfully started, it is optionally possible to check the status via the REST interface: 3.3

```
1 # GET PROXY STATUS
2 $ wget http://proxyinstance.local:5556/proxy/status
3 {
4 "capabilities": [
5   "static",
6   "axis_b",
7   "axis_x",
8   "axis_y",
9   "axis_z",
10  "axis_temp",
11  "axis_stimestamp"
12 ],
13 "commands": [
14   "status",
15   "initialize",
16   "disconnect",
17   "combinedsensorcnt",
18   "sensorcnt",
19   "readsensor",
20   "temp"
21 ]}
22 # RUN A SENSOR COMMAND AND GET THE TOTAL SENSOR COUNT
23 $ wget http://proxyinstance.local:5556/proxy/command?cmd=
```

```
combinedsensorcnt
24 {
25 "output": [
26   "2"
27 ]}
```

Listing 3.3: MRPPProxy REST endpoint query examples

The query result shows that the sensors are connected correctly and that their capabilities have also been recognised correctly. To be able to configure a measurement on the *control* PC, only the Internet Protocol (IP) address or hostname of the PC running an *MRPPProxy* instance is required 3.4.

```
1 # CONFIGURE MEASUREMENT JOB USING A PROXY INSTANCE
2 $ MRPcli config setsensor testcfg --path http://proxyinstance.local
   :5556
3 > remote sensor connected: True using proxy connection:
4 > http://proxyinstance.local:5556 with 1 local sensor connected
```

Listing 3.4: MRPcli usage example to connect with a network sensor

#### 3.3.2 Sensor Synchronisation

Another important aspect when using several sensors via the proxy system is the synchronisation of the measurement intervals between the sensors. Individual sensor setups do not require any additional synchronisation information, as this is communicated via the USB interface.

If several sensors are connected locally, they can be connected to each other via their sync input using short cables. One sensor acts as the central clock as described in 2.4.2. this no longer works for long distances and the synchronisation must be made via a shared network connection.

If time-critical synchronisation over the network is required, Precision Time Protocol (PTP) and Puls Per Second (PPS) output functionality [12] can be used on many SBC, such as the *Raspberry-Pi Compute Module*.

### 3.3.3 Command-Router

As it is possible to connect many identical sensors to one host, it must be possible to address them separately. This separation is done by the *MRPProxy* module and is a separate part from the core MRP-library, to keep installation package dependencies small.

Each connected sensor is accessed via the text-based CLI, this is initially the same for each sensor. The only identification feature is the sensor UUID by using the *id* command of the sensor CLI.

The *MRPProxy* instance claims to be a sensor to the host PC running MRP CLI, so the multiple sensors must be combined into one virtual one. This is done in several steps, start procedure described by the following sub-chapters.

#### Construct the Sensor ID LookUp-Table

Immediately after starting the *MRPProxy*, the UUIDs of all locally connected sensors are read out. These are stored together with the class instance of the *MRPHal* module in a LUT. This makes it possible to address a sensor directly using its UUID.

#### Merging the Sensor Capabilities

---

Table 3.1: Sensor capabilities merging algorithm

---

SENSOR A	SENSOR B	MERGED CAPABILITIES	CAPABLE SENSORS ID LUT
static	static		A
	dynamic	dynamic	B
axis_temp	axis_temp	axis_temp	A B
axis_x	axis_x	axis_x	A B

---

When using sensors with different capabilities, these must be combined. These are used to select the appropriate measurement mode for a measurement. For this purpose, the *info* command of each sensor is queried. This information is added to the previously created LUT. Duplicate entries are summarised (see Table 3.1) and returned to the host when the *info* 3.5 command is received over network.

```
1 # QUERY Network-Proxy capabilities
2 $ wget http://proxyinstance.local:5556/proxy/status
3 { "capabilities": [
4 "static",
5 "dynamic",
6 "axis_temp",
7 "axis_x"
8 ]}
```

Listing 3.5: MRPproxy REST endpoint query examples

The same procedure is performed for the *commands* CLI-command of each sensor, to merge available commands of connected sensors into the LUT.

#### Dynamic extension of the available Network-Proxy Commands

In order for the host to be able to send a command to the network multi-sensor setup, the command received must be forwarded to the correct sensor. In addition, there are commands such as the previously used *info* or *status* command, which must be intercepted by the *MRPProxy* module so that it can be handled differently (see example 3.5).

To realize this, a LUT is created in the previous steps, which contains information regarding *requested capability* -> *sensor-UUID* -> *physical sensor* and allows the commands to be routed.

For commands where there are several entries for *CAPABLE SENSORS ID LUT* 3.1, there are two possible approaches to how the command is processed:

- Redirect to each capable sensor
- Extend commands using an id parameter

These two methods have been implemented and are applied automatically. The decision is based on which hardware sensors are connected. In a setup where only the same

sensor variants are connected, *redirect to each capable sensor* is applied. This offers a time advantage as fewer commands need to be sent from the host. Thus, with a *readsensor* command, all sensors are read out via one command and the summarized result is transmitted to the host.

The *extend commands using an id parameter* strategy is used for different sensors. Each command is extended on the *Network-Proxy* 3.3.1 by another UUID parameter, according to the following scheme:

- *readsensor* -> *readsensor*
- *opmode* -> *opmode*

This allows the host to address individual sensors directly via their specific UUID.

## 3.4 Examples

The following shows some examples of how the MRP-library can be used. These examples are limited to a functional minimum for selected modules of the MRP-library. The documentation 4.4.1 contains further and more detailed examples. Many basic examples are also supplied in the form of the test scripts used for testing 4.3.

### 3.4.1 MRPRReading

The *MRPRReading* is the key module of the MRP core. It is used to manage the measurement data and can be imported and exported. The following example 3.6 shows how a measurement is created and measurement points are added in the form of *MRPRReadingEntry* instances.

An important point is the management of the meta data, which further describes the measurement. This is realised in the example using the *set\_additional\_data* function.

```
1 from MRP import MRPRReading, MRPMeasurementConfig
2 # [OPTIONAL] CONFIGURE READING USING MEASUREMENT CONFIG INSTANCE
3 config : MRPMeasurementConfig = MRPMeasurementConfig
4 config.sensor_distance_radius(40) # 40mm DISTANCE BETWEEN MAGNET AND
      SENSOR
```

```
5 config.magnet_type(N45_CUBIC_12x12x12) # CHECK MRPMagnetTypes.py FOR
   IMPLEMENTED TYPES
6 # CREATE READING
7 reading: MRPReading = MRPReading(config)
8 # ADD METADATA
9 reading.set_name("example reading")
10 ## ADD FURTHER DETAILS
11 reading.set_additional_data("description", "abc")
12 reading.set_additional_data("test-number", 1)
13 # INSERT A DATAPOINT
14 measurement = MRPReadingEntry.MRPReadingEntry()
15 measurement.value = random.random()
16 reading.insert_reading_instance(measurement, False)
17 # USE MEASURED VALUES IN OTHER FRAMEWORKS / DATAFORMATS
18 ## NUMPY
19 npmatrix: np.ndarray = reading.to_numpy_matrix()
20 ## CSV
21 csv: [] = reading.to_value_array()
22 ## JSON
23 js: dict = reading.dump()
24 # EXPORT READING TO FILE
25 reading.dump_to_file("exported_reading.mag.json")
26 # IMPORT READING
27 imported_reading: MRPReading = MRPReading()
28 imported_reading.load_from_file("exported_reading.mag.json")
```

Listing 3.6: MRPReading example for setting up an basic measurement

Finally, the measurement is exported for archiving and further processing; various export formats are available. Using the *dump\_to\_file* function, the measurement can be converted into an open JSON format.

#### 3.4.2 MRPHal

After generating simple measurements with random values in the previous example 3.4.1, the next step is to record real sensor data. For this purpose, the *MRPHal* module is developed, which can interact with all *Unified Sensor* 2-compatible sensors. In the following example 3.7, an *1D: Single Sensor* 2.5.1 is connected locally to the host PC.

```
1 from MRP import MRPHalSerialPortInformation, MRPHal, MRPBaseSensor,
   MRPHalReadingSource
2 # SEARCH FOR CONNECTED SENSORS
3 ## LISTS LOCAL CONNECTED OR NETWORK SENSORS
```

```
4 system_ports = MRPHalSerialPortInformation.list_sensors()
5 sensor = MRPHal(system_ports[0])
6 # OR USE SPECIFIED SENSOR DEVICE
7 device_path = MRPHalSerialPortInformation("UNFSensor1")
8 sensor = MRPHal(device_path)
9 # RAW SENSOR INTERACTION MODE
10 sensor.connect()
11 basesensor = MRPBaseSensor.MRPBaseSensor(sensor)
12 basesensor.query_readout()
13 print(basesensor.get_b()) # GET RAW MEASUREMENT
14 print(basesensor.get_b(1)) # GET RAW DATA FROM SENSOR WITH ID 1
15 # TO GENERATE A READING THE perform_measurement FUNCTION CAN BE USED
16 reading_source = MRPRReadingSourceHelper.createReadingSourceInstance(
    sensor)
17 result_readings: [MRPReading] = reading_source.perform_measurement(
    _readings=1, _hwavg=1)
```

Listing 3.7: MRPHal example to use an connected hardware sensor to store readings inside of a measurement

In general, a sensor can be connected using its specific system path or the sensor-UUID via the *MRPHalSerialPortInformation* function. Locally connected or network sensors can also be automatically recognised using the *list\_sensors* function. Once connected, these are then converted into a usable data source using the *MRPRReadingSource* module. This automatically recognises the type of sensor and generated an *MRPReading* instance with the measured values of the sensor.

#### 3.4.3 MRPSimulation

If no hardware sensor is available or for the generation of test data, the *MRPSimulation* module is available. This contains a series of functions that simulate various magnets and their fields. The result is a complete *MRPReading* measurement with a wide range of set meta data.

The example 3.8 illustrated the basic usage. Different variations of the *generate\_reading* function offers the user additional parameterisation options, such as random polarisation direction or a defined centre-of-gravity vector. The data is generated in the background using the *magpylib* [25] library according to the specified parameters.

```
1 from MRP import MRPSimulation, MRPPolarVisualization, MRPRReading
2 # GENERATE SULUMATED READING USING A SIMULATED HALLSENSOR FROM magpy
```

```
LIBRARY
3 reading = MRPSimulation.generate_reading(MagnetType.N45_CUBIC_12x12x12,
    _add_random_polarisation=True)
4 # GENERATE A FULLSPHERE MAP READING
5 reading_fullsphere = MRPSimulation.generate_random_full_sphere_reading()
6 # RENDER READING TO FILE IN 3D
7 visu = MRPPolarVisualization(reading)
8 visu.plot3d(None)
9 visu.plot3d("simulated_reading.png")
10 # EXPORT READING
11 reading.dump_to_file("simulated_reading.mag.json")
```

Listing 3.8: MRPSimulation example illustrates the usage of several data analysis functions

#### 3.4.4 MRPAnalysis

Once data can be acquired using hardware or software sensors, the next step is to analyse this data. MRP provides some simple analysis functions for this purpose. The code example shows the basic use of the module. The *Evaluation* 6 chapter shows how the user can implement their own algorithms and add them to the library.

```
1 from MRP import MRPAnalysis, MRPReading
2 # CREATE A SAMPLE MEASUREMENT WITH SIMULATED DATA
3 reading = MRPSimulation.generate_reading(MagnetType.N45_CUBIC_10x10x10)
4 # CALCULATE MEAN
5 print(MRPAnalysis.calculate_mean(reading))
6 # CALCULATE STD DEVIATION ON TEMPERATURE AXIS
7 print(MRPAnalysis.calculate_std_deviation(reading, _temperature_axis=
    True))
8 # CALCULATE CENTER OF GRAVITY
9 (x, y, z) = MRPAnalysis.calculate_center_of_gravity(reading)
10 # APPLY CALIBRATION READING TO REMOVE BACKGROUND NOISE
11 calibration_reading = MRPSimulation.generate_reading(MagnetType.
    N45_CUBIC_10x10x10, _ideal = True)
12 MRPAnalysis.apply_calibration_data_inplace(calibration_reading, reading
    )
```

Listing 3.9: MRPAnalysis example code performs several data analysis steps

### 3.4.5 MRPVisualisation

This final example shows the use of the *MRPVisualisation* module, which provides general functions for visualising measurements. The visualisation options make it possible to visually assess the results of a measurement. This is particularly helpful for full-sphere measurements recorded with the *3D: Fullsphere ??* sensor. The sub-module *MRPPolarVisualisation* is specially designed for these. The figure 3-4 shows a plot of a fullsphere measurement. It is also possible to export the data from the *MRPAnalysis* module graphically as diagrams. The *MRPVisualisation* modules are used here. The following example 3.10 shows the usage of both modules.

```
1 from MRP import MRPPolarVisualization
2 # CREATE MRPPolarVisualization INSTANCE
3 ## IT CAN BE REUSED CALLING plot2d AGAIN, AFTER LINKED READING DATA
4 visu = MRPPolarVisualization.MRPPolarVisualization(reading)
5 # 2D PLOT INTO A WINDOW
6 visu.plot2d_top(None)
7 visu.plot2d_side(None)
8 # 3D PLOT TO FILE
9 visu.plot3d(os.path.join('./plot3d_3d.png'))
10 # PLOT ANALYSIS RESULTS
11 from MRP import MRPDataVisualization
12 MRPDataVisualization.MRPDataVisualization.plot_error([reading_a,
    reading_b, reading_c])
```

Listing 3.10: MRPVisualisation example which plots a fullsphere to an image file

### 3.4.6 MRPHalbachArrayGenerator

The following example code 3.11, shows how a simple Halbach magnetic ring can be generated.

This can then be used to construct a Halbach ring magnet (see chapter 1.1.2) for a low-field MRI.

Eight random measurements are generated here. It is important that the magnet type (for example *N45\_CUBIC\_15x15x15*) is specified. This is necessary so that the correct magnet cutouts can be generated when creating the 3D model.

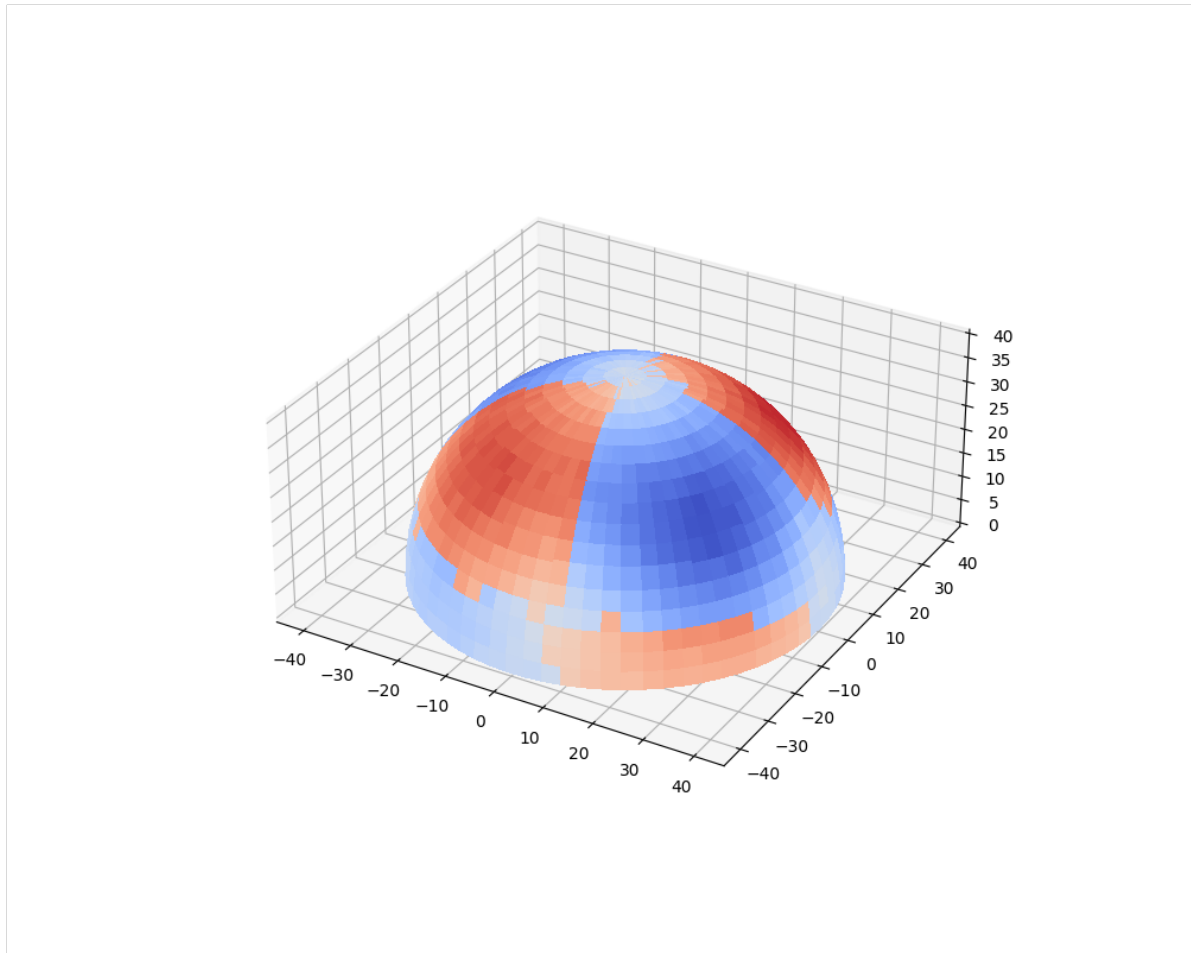


**Figure 3-4:** Example full sphere plot of an measurement using the MRPVisualisation module

### 3 Software Readout Framework

---

After the measurements have been generated, they are provided with a position and rotation offset according to the Halbach design and calculation scheme [26] using the *MRPHalbachArrayGenerator* module.

```
1 readings = []
2 for idx in range(8):
3     # GENERATE EXAMPLE READINGS USING N45 CUBIC 15x15x15 MAGNETS
4     readings.append(MRPSimulation.MRPSimulation.generate_reading(
5         MRPMagnetTypes.MagnetType.N45_CUBIC_15x15x15))
6 ## GENERATE HALBACH
7 halbach_array: MRPHalbachArrayGenerator.MRPHalbachArrayResult =
8     MRPHalbachArrayGenerator.MRPHalbachArrayGenerator.
9         generate_1k_halbach_using_polarisation_direction(readings)
10 # EXPORT TO OPENSCAD
11 ## 2D MODE DXF e.g. for lasercutting
12 MRPHalbachArrayGenerator.MRPHalbachArrayGenerator.
13     generate_openscad_model([halbach_array], "./2d_test.scad",
14     _2d_object_code=True)
15 ## 3D MODE e.g. for 3D printing
16 MRPHalbachArrayGenerator.MRPHalbachArrayGenerator.
17     generate_openscad_model([halbach_array], "./3d_test.scad",
18     _2d_object_code=False)
```

Listing 3.11: *MRPHalbachArrayGenerator* example for generating an OpenSCAD based halbach ring

In the last step, a 3D model with the dimensions of the magnet type set is generated from the generated magnet positions. The result is an *OpenSCAD* [18] file, which contains the module generated. After computing the model using the *OpenSCAD* CLI utility, the following model rendering 3-5 can be generated.

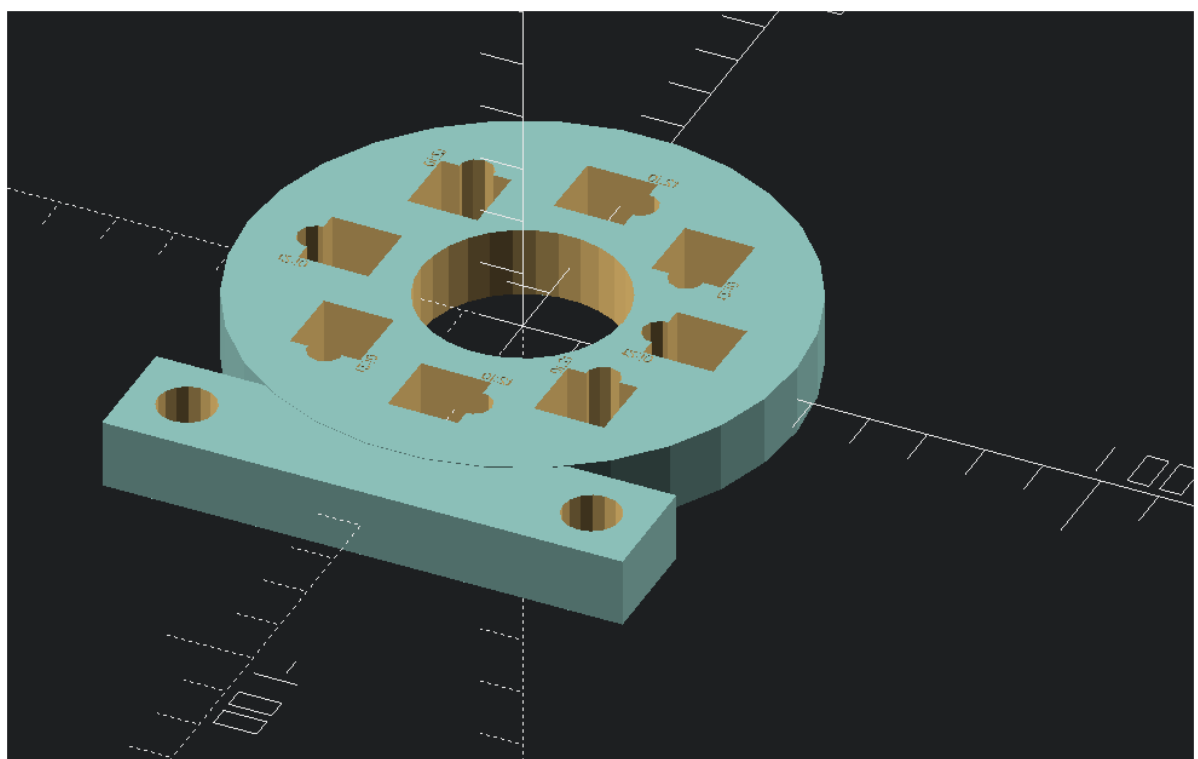


Figure 3-5: Generated Hallbach array with generated cutouts for eight magnets

# 4 Usability Improvements

Usability improvements in software libraries are essential for efficient and user-friendly development. Intuitive API documentation, clearly structured code examples and improved error messages promote a smooth developer experience. A Graphical User Interface (GUI) or CLI application for complex libraries can make it easier to use, especially for developers with less experience. Continuous feedback through automated tests and comprehensive error logs enable faster bug fixing.

The integration of user feedback and regular updates promotes the adaptability of the MRP-library. Effective usability improvements help to speed up development processes and increase the satisfaction of the developer community. In the following, some of these have been added in and around the MRP-library, but they are only optional components for the intended use.

## 4.1 Command Line Interface

In the first version of the MRP-library, the user had to write his own Python scripts even for short measurement and visualisation tasks. This is already a time-consuming process for reading out a sensor and configuring the measurement parameters and metadata and quickly required more than 100 lines of new Python code.

```
CONFIGURE READING
READING-NAME: [read_dualsensor_normal]: >? new_measurement
OUTPUT-FOLDER [./readings/tlv493d_N45_12x12x12/] : >? ./
final output path for reading /Users/marcelochsendorf/Downloads/MagneticReadoutProcessing/src/MagneticReadoutProcessing
SUPPORTED MAGNET TYPES
0 > NOT_SPECIFIED
1 > RANDOM_MAGNET
2 > N45_CUBIC_12x12x12
3 > N45_CUBIC_15x15x15
4 > N45_CUBIC_9x9x9
5 > N45_CYLINDER_5x10
6 > N45_SPHERE_10
Please select one of the listed magnet types [0-6] [2]:
>? 3
```

Figure 4-1: MRP CLI output to configure a new measurement

Although such examples are provided in the documentation, it must be possible for programming beginners in particular to use them. To simplify these tasks, a CLI 4-2 is implemented. The library CLI implements the following functionalities:

- Detection of connected sensors
- Configuration of measurement series
- Recording of measured values from stored measurement series
- Simple commands for checking recorded measurement series and their data

Thanks to this functionality of the CLI, it is now possible to connect a sensor to the PC, configure a measurement series with it and run it at the end. The result is an exported file with the measured values. These can then be read in again using the *MRPReading* module and processed further. The following bash code 4.1 shows the setup procedure in detail:

```
1 # CLI EXAMPLE FOR CONFIGURING A MEASUREMENT RUN
2 ## CONFIGURE THE SENSOR TO USE
3 $ MRPcli config setupsensor testcfg
4 > 0 - Unified Sensor 386731533439 - /dev/cu.usbmodem3867315334391
5 > Please select one of the found sensors [0]:
6 > sensor connected: True 1243455
7 ## CONFIGURE THE MEASUREMENT
8 $ MRPcli config setup testcfg
9 > CONFIGURE testcfg
10 > READING-NAME: [testreading]: testreading
11 > OUTPUT-FOLDER [/cli/reading]: /tmp/reading_folder_path
12 > NUMBER DATAPOINTS: [1]: 10
13 > NUMBER AVERAGE READINGS PER DATAPOINT: [1]: 100
14 # RUN THE CONFIGURED MEASUREMENT
15 $ MRPcli measure run
16 > STARTING MEASUREMENT RUN WITH FOLLOWING CONFIGS: ['testcfg']
17 > config-test: OK
18 > sensor-connection-test: OK
19 > START MEASUREMENT CYCLE
20 > sampling 10 datapoints with 100 average readings
21 > SID:0 DP:0 B:47.359mT TEMP:23.56
22 > ....
23 > dump_to_file testreading_ID:525771256544952_SID:0_MAG:
    N45_CUBIC_12x12x12.mag.json
```

Listing 4.1: CLI example for configuring a measurement run

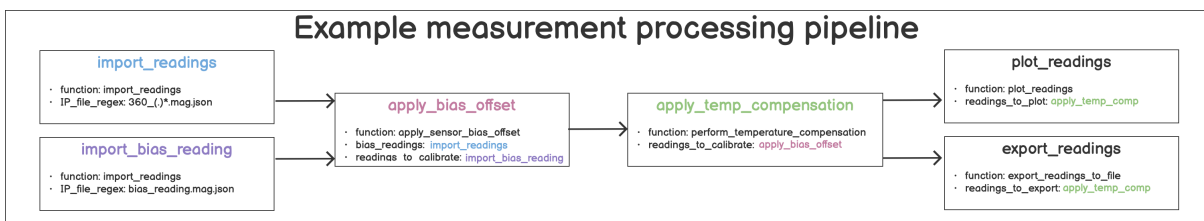


Figure 4-2: Example measurement analysis pipeline

## 4.2 Programmable Data Processing Pipeline

After it is easy for users to carry out measurements using the CLI, the next logical step is to analyse the recorded data. This can involve one or several hundred data records. Again, the procedure for the user is to write their own evaluation scripts using the MRP-library.

This is particularly useful for complex analyses or custom algorithms, but not necessarily for simple standard tasks such as bias compensation or graphical plot outputs.

For this purpose, a further CLI application is created, which enables the user to create and execute complex evaluation pipelines for measurement data without programming. The example 4-2 shows a typical measurement data analysis pipeline, which consists of the following steps:

1. Import the measurements
2. Determine sensor bias value from imported measurements using a reference measurement
3. Apply linear temperature compensation
4. Export the modified measurements
5. Create a graphical plot of all measurements with standard deviation

In order to implement such a pipeline, the *yaml* file format is chosen for the definition of the pipeline, as this is for non programmers to understand and can also be easily edited with a plain text editor. Detailed examples can be found in the documentation [5]. The pipeline definition consists of sections which execute the appropriate Python commands in the background.

The signatures in the *yaml* file are called using reflection and a real-time search of the loaded *global()* functions symbol table [9]. This system makes almost all Python functions available to the user. To simplify use, a pre-defined list of verified functions for

use in pipelines is listed in the documentation [5]. The following pipeline definition 4.2 shows the previously defined steps 4-2 as *yaml* syntax.

```
1 stage import_readings:
2   function: import_readings
3   parameters:
4     IP_input_folder: ./readings/fullsphere/
5     IP_file_regex: 360_(.)*.mag.json
6
7 stage import_bias_reading:
8   function: import_readings
9   parameters:
10    IP_input_folder: ./readings/fullsphere/
11    IP_file_regex: bias_reading.mag.json
12
13 stage apply_bias_offset:
14   function: apply_sensor_bias_offset
15   parameters:
16     bias_readings: stage import_bias_reading # USE RESULT FROM FUNCTION
17       import_bias_reading
17     readings_to_calibrate: stage import_readings
18
19 stage apply_temp_compensation:
20   function: apply_temperature_compensation
21   parameters:
22     readings_to_calibrate: stage import_readings # USE RESULT FROM
23       FUNCTION import_readings
23
24 stage plot_normal_bias_offset:
25   function: plot_readings
26   parameters:
27     readings_to_plot: stage apply_temp_compensation
28     IP_export_folder: ./readings/fullsphere/plots/
29     IP_plot_headline_prefix: Sample N45 12x12x12 magnets calibrated
30
31 stage export_readings:
32   function: export_readings
33   parameters:
34     readings_to_plot: stage apply_temp_compensation
35     IP_export_folder: ./readings/fullsphere/plots/
```

Listing 4.2: Example YAML code of an user defined processing pipeline with six stages linked together

Each pipeline step is divided into *stages*, which contain a name, the function to be executed and its parameters.

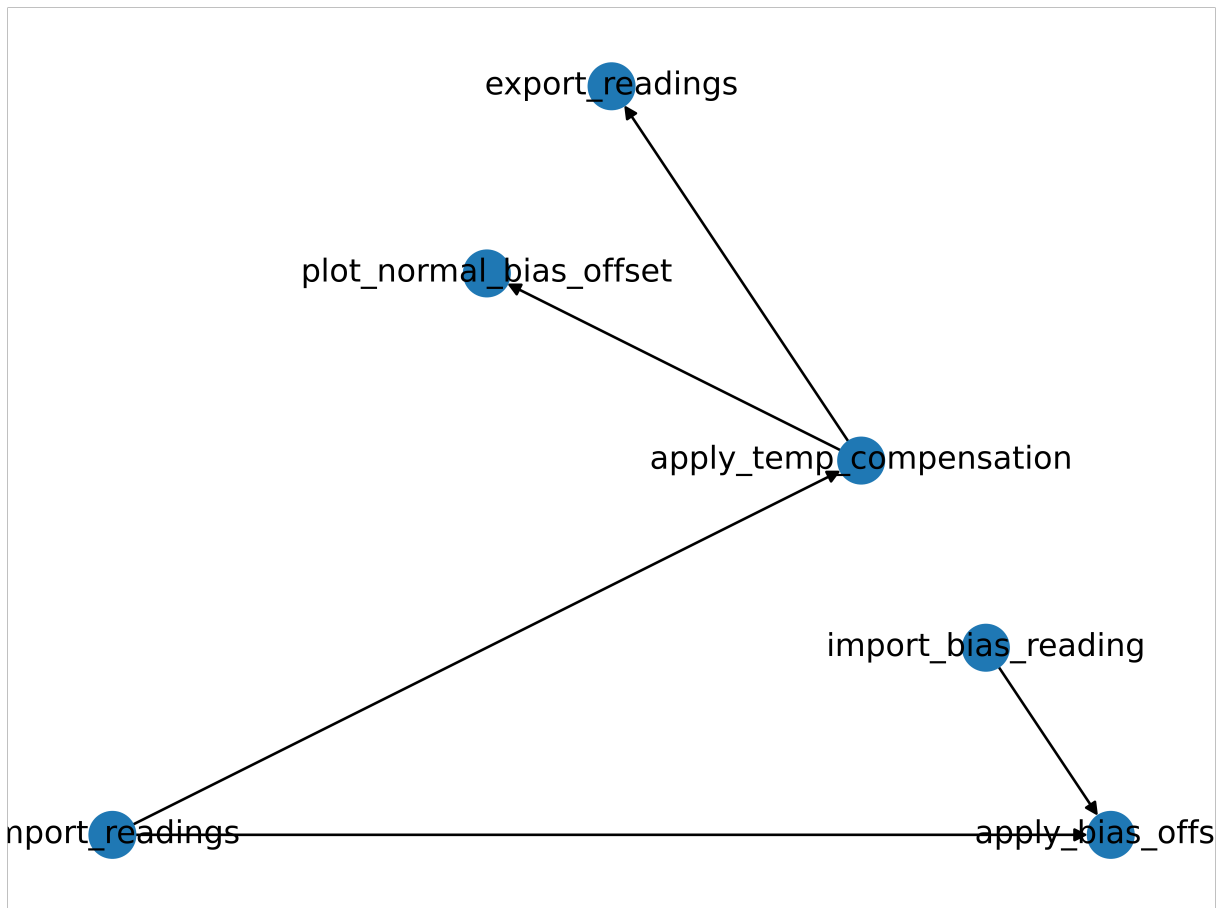


**Figure 4-3:** Example result of an step execution tree from user defined processing pipeline

The various steps are then linked by using the `stage` makro as input parameter of the next function to be executed (see comments in 4.2).

It is therefore also possible to use the results of one function in several others without them directly following each other. The disadvantages of this system are the following:

- No circular parameter dependencies
- Complex determination of the execution sequence of the steps

To determine the order of the pipeline steps, the parser script created converts them into one problem of the graph theories. Each step represents a node in the graph and the steps referred to by the input parameter form the edges. After several simplification steps, determination of possible start steps and repeated traversal, the final execution sequence can be determined in the form of a call tree 4-3. The individual steps are then executed along the graph. The intermediate results and the final results 4-4 are saved for optional later use.

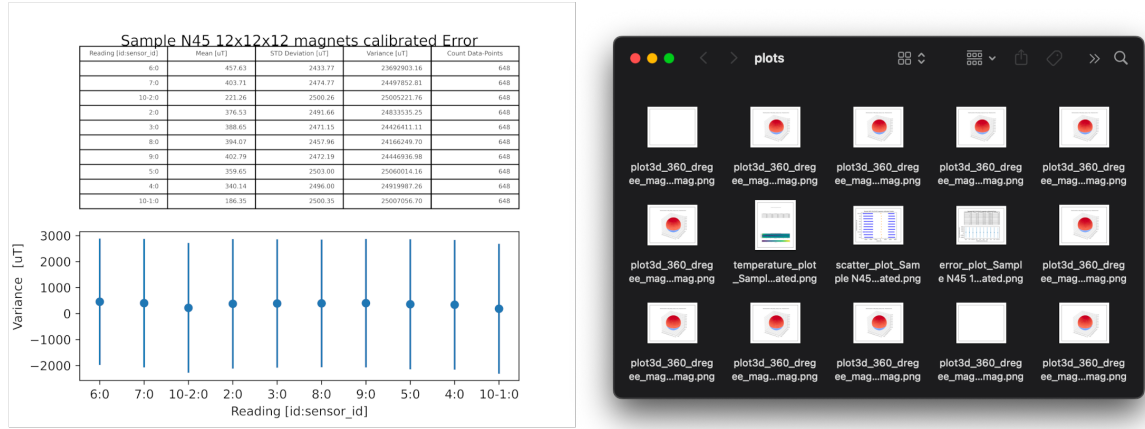


Figure 4-4: Pipeline output files after running example pipeline on a set of readings

```

test_MRPReading
  ✓ TestMPRReading
    ✓ test_cartesian_reading      0 ms
    ✓ test_export_reading        7 ms
    ✓ test_import_reading       0 ms
    ✓ test_matrix_init          372 ms
    ✓ test_reading_init         2 ms
  >  test_MPReadoutSource      0 ms
  ⚡ test_MRPSimulation        0 ms
  ✓ test_SensorAnalysis
    ✓ TestMRPDataVisualization  15 sec 850 ms
      ✓ test_error_visualisation 3 sec 72 ms
      ✓ test_mean                0 ms
      ✓ test_scatter_visualisation 2 sec 876 ms
      ✓ test_std_deviation       0 ms
      ✓ test_temperature_visualisation 9 sec 902 ms
    Skipped
    SKIPPED [ 79%]
    Skipped
    SKIPPED [ 82%]
    Skipped
    test_SensorAnalysis.py::TestMRPDataVisualization::test_mean
    test_SensorAnalysis.py::TestMRPDataVisualization::test_scatter_visualisation
    test_SensorAnalysis.py::TestMRPDataVisualization::test_std_deviation
    test_SensorAnalysis.py::TestMRPDataVisualization::test_temperature_visualisation
    test_SensorAnalysis.py::TestMRPDataVisualization::test_variance
    test_misc.py::TestMRPReading::test_full_sphere_reading PASSED [ 84%]PASSED [ 87%]PASSED [ 89%]PASSED [ 92%]PASSED [ 94%]
=====
===== 2 failed, 22 passed, 15 skipped, 13 warnings in 49.36s =====
PASSED [100%]
Process finished with exit code 1

```

Figure 4-5: MRP library test results for different submodules executed in PyCharm Integrated Development Environment (IDE)

### 4.3 Testing

Software tests in libraries offer numerous advantages for improving quality and efficiency. Software tests make it possible to identify errors and vulnerabilities before the software is released as a new version.

This significantly improves the reliability of MRP-library applications. Tests also ensure consistent and reliable performance, which is particularly important when libraries are used by different users and for different usecases.

During the development of the MRP-library, test cases were also created for all important functionalities and usecases. The test framework *PyTest* [19] is used for this purpose, as it offers direct integration in most IDEs (see 4-5) and also because it provides detailed and easy-to-understand test reports as output in order to quickly identify and correct errors. It also allows to tag tests, which is useful for grouping tests or excluding certain tests in certain build environment scenarios. Since all intended usecases were mapped

using the test cases created, the code of the test cases could later be used in slightly simplified variants 4.3 as examples for the documentation.

```

1 class TestMPRReading(unittest.TestCase) :
2     # PREPARE A INITIAL CONFIGURATION FILE FOR ALL FOLLOWING TEST CASES
3     # IN THIS FILE
4     def setUp(self) -> None:
5         self.test_folder: str = os.path.join(os.path.dirname(os.path.
6             abspath(__file__)), "tmp")
7         self.test_file:str = os.path.join(self.
8             import_export_test_folderpath, "tmp")
9
10    def test_matrix(self):
11        reading: MRPReading = MRPSimulation.generate_reading()
12        matrix: np.ndarray = reading.to_numpy_matrix()
13        n_phi: float = reading.measurement_config.n_phi
14        n_theta: float = reading.measurement_config.n_theta
15        # CHECK MATRIX SHAPE
16        self.assertTrue(matrix.shape != (n_theta,))
17        self.assertTrue(len(matrix.shape) <= n_phi)
18
19    def test_export_reading(self) -> None:
20        reading: MRPReading = MRPSimulation.generate_reading()
21        self.assertIsNotNone(reading)
22        # EXPORT READING TO A FILE
23        reading.dump_to_file(self.test_file)
24
25    def test_import_reading(self):
26        # CREATE EMPTY READING AND LOAD FROM FILE
27        reading_imported:MRPReading = MRPReading.MRPReading(None)
28        reading_imported.load_from_file(self.test_file)
29        # COMPARE
30        self.assertIsNotNone(reading_imported.compare(MRPSimulation.
31            generate_reading()))

```

Listing 4.3: Example pytest class for testing MRPReading module functions

One problem, is the parts of the MRP-library that require direct access to external hardware. These are, for example, the *MRPHal* and *MRPHalRest* modules, which are required to read out sensors connected via the network. Two different approaches were used here. In the case of local development, the test runs were carried out on a PC that can reach the network hardware and thus the test run could be carried out with real data.

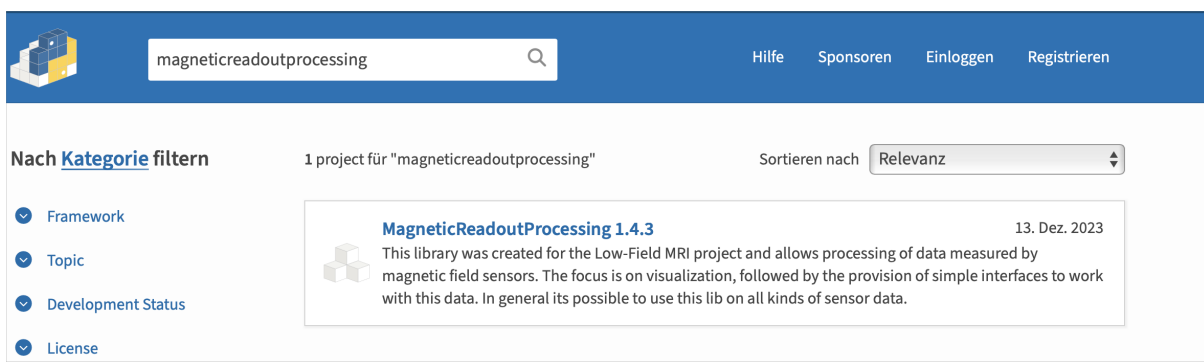


**Figure 4-6:** MagneticReadoutProcessing library hosted on PyPi

In the other scenario, the tests are to be carried out before a new release in the repository on the basis of *Github Actions* [13]. Here there is the possibility to host local runner software, which then has access to the hardware, but then a PC must be permanently available for this task. Instead, the hardware sensors were simulated by software and executed via virtualisation on the systems provided by *Github Actions*.

## 4.4 Package Distribution

One important point that improves usability for users is the simple installation of all MRP modules. As it is created in the Python programming language, there are several public package registry where users can provide their software modules. Here, *PyPi* [8] 4-6 [7] is the most commonly used package registry and offers direct support for the package installation program Python Package Installer (PIP) 4.4.

PIP not only manages possible package dependencies, but also manages the installation of different versions of a package. In addition, the version compatibility is also checked during the installation of a new package, which can be resolved manually by the user in the event of conflicts.

```

1 # https://pypi.org/project/MagneticReadoutProcessing/
2 # install the latest version
3 $ pip3 install MagneticReadoutProcessing
4 # install the specific version 1.4.0
5 $ pip3 install MagneticReadoutProcessing==1.4.0

```

**Listing 4.4:** Bash commands to install the MagneticReadoutProcessing library using pip

To make the MRP file structure compatible with the package registry, Python provides

separate installation routines that build a package in an isolated environment and then provide an installation *wheel* archive. This can then be uploaded to the package registry. Since the MRP-library requires additional Python dependencies, which cannot be assumed to be already installed on the target system, these must be installed prior to the actual installation. These can be specified in the library installation configuration *setup.py* 4.5 for this purpose.

```
1 # dynamic requirement loading using 'requirements.txt'
2 req_path = './requirements.txt'
3 with pathlib.Path(req_path).open() as requirements_txt:
4     install_requires = [str(requirement) for requirement in pkg_resources
5                         .parse_requirements(requirements_txt)]
6
7 setup(name='MagneticReadoutProcessing',
8       version='1.4.3',
9       url='https://github.com/LFB-MRI/MagnetCharacterization/',
10      packages=['MRP', 'MRPcli', 'MRPUDpp', 'MRPproxy'],
11      install_requires=install_requires,
12      entry_points={
13          'console_scripts': [
14              'MRPcli = MRPcli.cli:run',
15              'MRPUDpp = MRPUDpp.udpp:run',
16              'MRPproxy = MRPproxy.mrpproxy:run'
17          ]
18      }
19 )
```

Listing 4.5: *setup.py* with dynamic requirement parsing used given *requirements.txt*

To make the CLI scripts written in Python easier for the user to execute without having to use the *python3* prefix. This has been configured in the installation configuration using the *entry\_points* option, and the following commands are available to the user:

- *\$ MRPcli –help* instead of *\$ python3 cli.py –help*
- *\$ MRPUDpp –help* instead of *\$ python3 udpp.py –help*
- *\$ MRPproxy –help* instead of *\$ python3 proxy.py –help*

In addition, these commands are available globally in the system without the terminal shell being located in the MRP-library folder.

#### 4.4.1 Documentation

In order to provide comprehensive documentation for the enduser, the source code is documented using Python-*docstrings* [11] and the Python type annotations. The use of type annotations also simplifies further development, as modern IDEs can more reliably display possible methods to the user as an assistance.

```
1 # MRPDataVisualisation.py – example docstring
2 def plot_temperature(_readings: [MRPReading.MRPReading], _title: str =
3     '', _filename: str = None, _unit: str = "degree C") -> str:
4     """
5         Plots a temperature bar graph of the reading data entries as figure
6         :param _readings: readings to plot
7         :type _readings: list(MRPReading.MRPReading)
8         :param _title: Title text of the figure , embedded into the head
9         :type _title: str
10        :param _filename: export graphic to an given absolute filepath with .
11            png
12        :type _filename: str
13        :returns: returns the abs filepath of the generated file
14        :rtype: str
15        """
16        if _readings is None or len(_readings) <= 0:
17            raise MRPDataVisualizationException("no readings in _reading
18                given")
19        num_readings = len(_readings)
20        # ...
```

Listing 4.6: Documentation using Python docstring example

Since *docstrings* only document the source code, but do not provide simple how-to-use instructions, the documentation framework *Sphinx* [4] is used for this purpose. This framework makes it possible to generate Hypertext Markup Language (HTML) or Portable Document Format (PDF) documentation from various source code documentation formats, such as the used *docstrings*.

These are converted into a Markdown format in an intermediate step and this also allows to add further user documentation such as examples or installation instructions. In order to make the documentation created by *Sphinx* accessible to the user, there are, as with the package management by *PyPi* services, which provide the MRP-library documentation online.

Once the finished documentation has been generated from static HTML files, it is stored

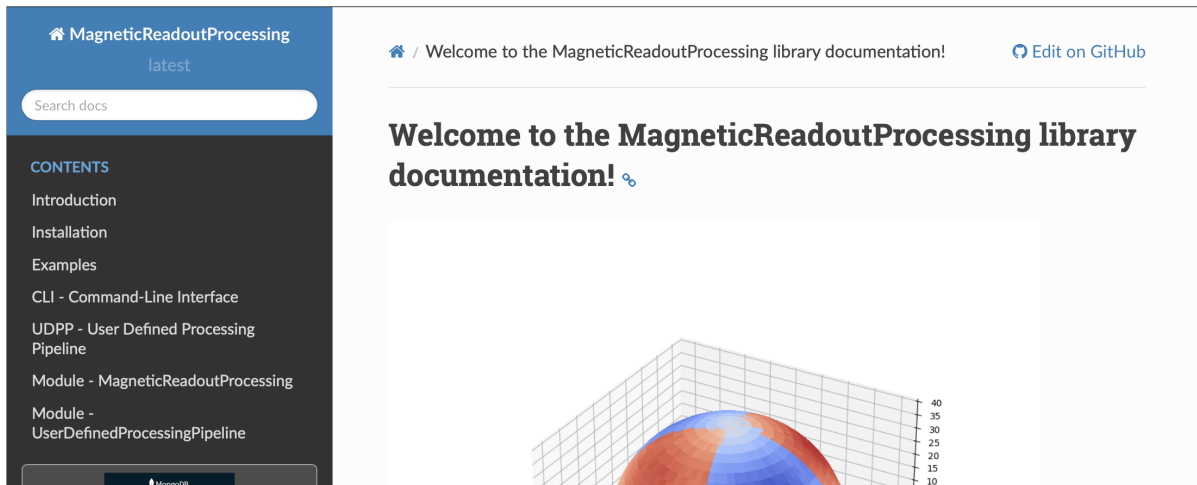


Figure 4-7: MagneticReadoutProcessing documentation hosted on ReadTheDocs

in the project repository. Another publication option is to host the documentation via online services such as *ReadTheDocs* [6], where users can make documentation for typical software projects available to others.

The documentation has also been uploaded to *ReadTheDocs* [5] and linked in the repository and on the overview page 4-7 on *PyPi*.

The process of creating and publishing the documentation has been automated using *GitHub Actions*, so that it is always automatically kept up to date with new features.

# 5 Usecase Evaluation

The practical application of the hardware and software framework is shown below. This is shown using the previously defined usecases 1.5. In the application example, various permanent magnets are measured and then sorted according to their field strength. The result should then list the magnets that deviate the least from each other in terms of their field strength. This is determined using a sorting algorithm developed by the user.

The process is broken down into the following steps and the practical application of *User Interaction Points* 3.1 is shown:

1. **Hardware preparation:** Users can prepare measurements using the implemented framework. This includes the placement of the sensors and the selection of the relevant parameters for the characterisation of the permanent magnets.
2. **Configuration of the measurement:** The software provides a user-friendly interface for configuring the measurement parameters. Users can make the desired settings here and customise the framework to their specific requirements.
3. **Custom algorithm implementation:** An important contribution of the MRP ecosystem is the possibility for users to implement their own algorithm for data analysis. This allows customisation to specific research questions or experimental requirements.
4. **Execution of analysis pipeline:** The analysis pipeline can then be executed with the implemented algorithm. The collected measurement data is automatically processed and analysed to extract characteristic parameters of the permanent magnets.

This process covers all the essential functionalities required for a comprehensive characterisation of permanent magnets. These were previously described in the Usecases

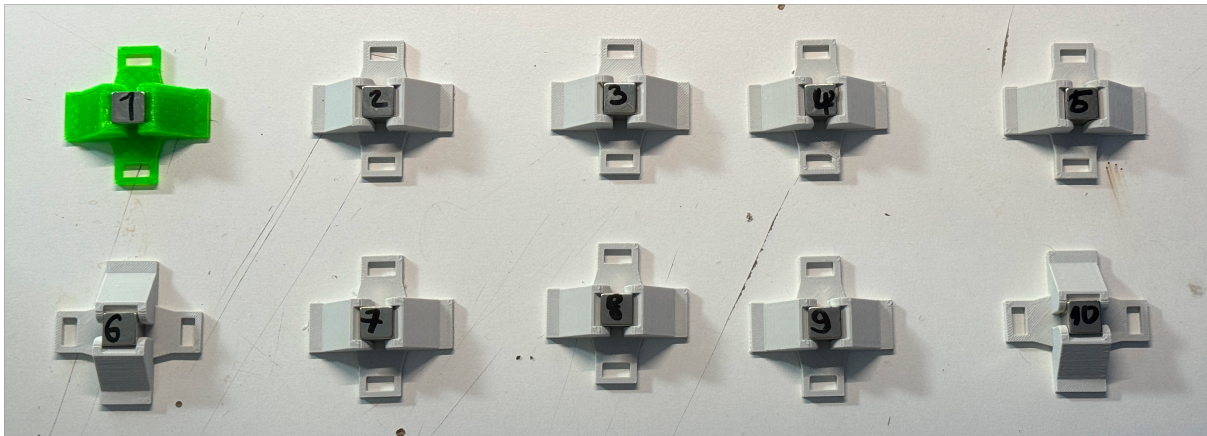


Figure 5-1: Ten numbered test magnets in separate holders

1.5 chapter. The developed framework not only offers a cost-effective and flexible hardware solution, but also enables customisation of the analysis algorithms to meet the requirements of different research projects.

## 5.1 Hardware preparation

For the hardware setup, the 3D-Fullsphere?? sensor is used for the evaluation of the framework. As this is equipped with an exchangeable magnetic holder mount, suitable holders are required for the magnets to be measured. Ten random  $N45\ 12x12x12mm$  neodymium magnets were used, which are shown in figure 5-1.

These were placed in modified 3D printed holders 5-1 and then numbered. This allows them to be matched to the measurement results later.

## 5.2 Configuration of the Measurement

The configured hardware is then connected to the host system using the *MRPcli config setupsensor*-CLI command. Afterwards, the measurement is configured for an measurement run, using the following configuration commands 5.1.

```
1 ## CONFIGURE THE MEASUREMENT
2 $ MRPcli config setup eval_measurement_config
3 > READING-NAME: 360_eval_magnet_<id>
4 > OUTPUT-FOLDER: ./readings/evaluation/
5 > NUMBER DATAPOINTS: 18 # FOR A FULLSPHERE READING USE MULTIPLE OF 18
6 > NUMBER AVERAGE READINGS PER DATAPPOINT: 10
```

Listing 5.1: Measurement configuration for evaluation measurement

The *MRPcli measure run* command is then called up for each individual magnet to execute a measurement. After each run, the *READING-NAME* parameter is filled with the id of the next magnet so that all measurements could be assigned to the physical magnets.

## 5.3 Custom Algorithm Implementation

The next step for the user is the implementation of the filter algorithm 5.2. This can have any function signature and is implemented in the file *UDPPFunctionCollection.py*. This Python file is loaded when the pipeline is started and all functions that are imported here as a module or implemented directly can be called via the pipeline. As this is a short algorithm, it is inserted directly into the file.

The parameter *\*\_readings\** should later receive the imported measurements from the stage *rawimport* 5.4 and the optional *IP\_return\_count* parameter specifies the number of best measurements that are returned. The return parameter is a list of measurements containing the most similar measurements, measured by the smallest distance between all measurements. The distance for each measurement is determined using the centre of gravity function *CoG*, the length is then calculated from the result vector. This value can then be used for sorting.

```
1 @staticmethod
2 def FindSimilarValuesAlgorithm(_readings: [MRPReading.MRPReading],
3                                 IP_return_count: int = -1) -> [MRPReading.MRPReading]:
4     import heapq
5     import math
6     heap = []
7     # SET RESULT VALUE COUNT
8     IP_return_count = max([int(IP_return_count), len(_readings)])
9     if IP_return_count < 0:
```

```

9     IP_return_count = len(_readings) / 5
10    # CALCULATE TARGET VALUE: CENTER OF GRAVITY MAGNITUDE FOR ALL
11    # READINGS
12    target_value = 0.0
13    for idx, r in enumerate(_readings):
14        cog = MRPAnalysis.MRPAnalysis.calculate_center_of_gravity(r)
15        # COMPUTE LENGTH OF VECTOR
16        cog_value: float = math.sqrt(cog[0]**2 + cog[1]**2 + cog[2]**2)
17        target_value = target_value + cog
18    target_value = target_value / len(_readings)
19    # PUSH READINGS TO HEAP
20    for value in _readings:
21        # USE DIFF AS PRIORITY VALUE IN MIN-HEAP
22        cog = MRPAnalysis.MRPAnalysis.calculate_center_of_gravity(value)
23        cog_value: float = math.sqrt(cog[0]**2 + cog[1]**2 + cog[2]**2)
24        diff = abs(cog_value - target_value)
25        heapq.heappush(heap, (diff, cog_value))
26    # RETURN X BEST ITEMS FROM HEAP
27    similar_values = [item[1] for item in heapq.nsmallest(IP_return_count,
28        heap)]
29    # CLEAN UP USED LIBRARIES AND RETURN RESULT
30    del heapq
31    del math
32    return similar_values

```

Listing 5.2: User implemented custom find most similar readings algorithm

The Python `heapq` [10] module, which implements a priority queue, is used for this purpose. The calculated distances from the *CoG* value of the measurements to are inserted into this queue. Subsequently, as many elements of the queue are returned as defined by the *IP\_return\_count* parameter. The actual sorting is carried out by the queue in the background.

### 5.3.1 Alternative Filter Algorithm Implementation

Another possibility here would be for the user to use a reference measurement instead of a simulated ideal magnet as a reference. This can come from a magnet selected as a reference magnet. As a result, the filter algorithm returns the measurements that are most similar to the selected reference magnet. The code snipped 5.3 shows the modified filter algorithm code, with added `*_ref*` input parameter for the reference measurement.

```

1 @staticmethod
2 def FindSimilarValuesAlgorithmREF(_readings: [MRPReading.MRPReading],
3                                     _ref: [MRPReading.MRPReading], IP_return_count: int = 4) -> [
4                                         MRPReading.MRPReading]:
5     # CALCULATE COG VALUE OF REFERENCE MAGNET
6     cog_ref = MRPAnalysis.MRPAnalysis.calculate_center_of_gravity(_ref[0])
7     ref_value: float = math.sqrt(cog_ref[0]**2 + cog_ref[1]**2 + cog_ref[2]**2)
8     # PUSH READINGS TO HEAP
9     for value in _readings:
10         # USE DIFF AS PRIORITY VALUE IN MIN-HEAP
11         cog = MRPAnalysis.MRPAnalysis.calculate_center_of_gravity(value)
12         cog_value: float = math.sqrt(cog[0]**2 + cog[1]**2 + cog[2]**2)
13         heapq.heappush(heap, (abs(cog_value - ref_value), cog_value))
14     # RETURN X BEST ITEMS FROM HEAP
15     return [item[1] for item in heapq.nsmallest(IP_return_count, heap)]

```

Listing 5.3: Modified user implemented custom find algorithm using a reference magnet reading

## 5.4 Execution of Analysis Pipeline

Once the filter function has been implemented, it still needs to be integrated into the analysis pipeline 5.4. Here, the example pipeline 4-2 is simplified and an additional stage *find\_similar\_values* has been added, which has set *FindSimilarValuesAlgorithm* as the function to be called. As a final step, the result is used in the *plot\_filtered* stage for visualisation.

```

1 settings:
2   enabled: true
3   export_intermediate_results: false
4   name: pipeline_mrp_evaluation
5
6 stage rawimport:
7   function: import_readings
8   parameters:
9     IP_input_folder: ./readings/evaluation/
10    IP_file_regex: 360_(.)*.mag.json
11
12 stage find_similar_values:
13   function: custom_find_similar_values_algorithm
14   parameters:

```

```

15     _readings: stage rawimport # USE RESULTS FROM rawimport STAGE
16     IP_return_count: 4 # RETURN BEST 4 of 10 READINGS
17
18 stage plot_filtered:
19   function: plot_readings
20   parameters:
21     readings_to_plot: stage find_similar_values # USE RESULTS FROM
22       find_similar_values STAGE
23     IP_export_folder: ./readings/evaluation/plots/plot_filtered/
24     IP_plot_headline_prefix: MRP evaluation - filtered

```

Listing 5.4: User defined processing pipeline using custom implemented filter algorithm

The final pipeline has been saved in the pipeline directory as *pipeline\_mrp\_evaluation.yaml* file and is ready for execution. This is carried out using the *MRPudpp* CLI 5.5. After the run has been successfully completed, the results are saved in the result folder specified in the pipeline using the *IP\_export\_folder* parameter.

```

1 # LIST ACTIVE PIPELINES IN PIPELINE DIRECTORY
2 $ MRPudpp pipeline listenabledpipelines
3 > Found enabled pipelines:
4 > 1. pipeline_mrp_evaluation.yaml
5 # EXECUTE THE EVALUATION PIPELINE
6 $ MRPudpp pipeline run
7 > loading pipeline pipeline_mrp_evaluation.yaml
8 > stage nodes: ['import', 'find_similar_values', 'plot_raw', '
    plot_filtered']
9 > =====> stage: import
10 > =====> stage: find_similar_values
11 > =====> stage plot_filtered
12 > Process finished with exit code 0

```

Listing 5.5: Bash result log of evaluation pipeline run

## 5.5 Result Analysis

The figure 5-2 shows this result. The plot of the raw measured values is shown on the left. The value of the determined *GoG*  $\mu$ T values is plotted on ten individual measured values. Here it can be seen that there are measured values with larger deviations (see measurement 7:0,10-2:0,10-1:0).

## 5 Usecase Evaluation

---

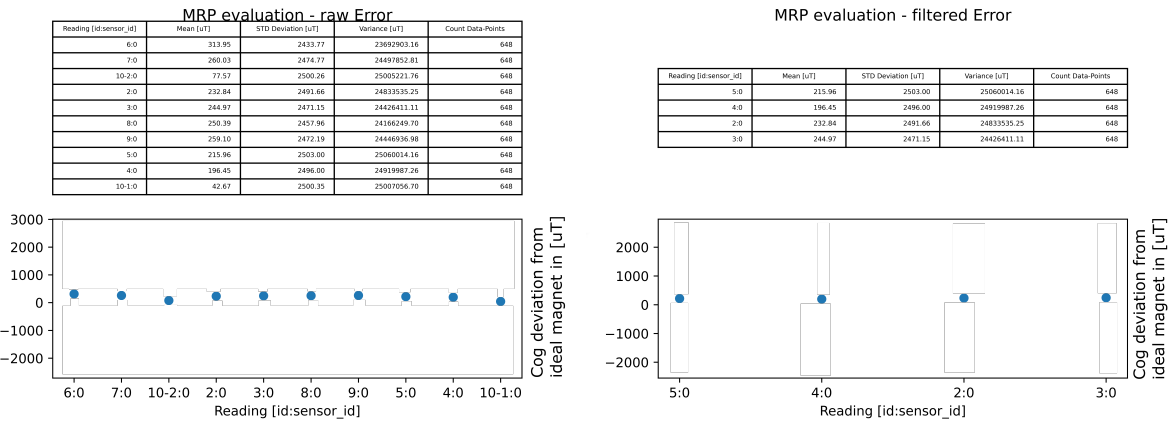


**Figure 5-2:** MRP evaluation result after execution of the user defined pipeline, using find similar values algorithm

On the right-hand side **5-2**, the measured values are plotted as a result of the filter algorithm. As the *IP\_return\_count* parameter is set to four, only the four most similar measurements were exported here. It can be seen from the plotted CoG  $\mu$ T deviation values, that these are closest to an ideal Magnet with a CoG value of  $0\mu$ T. This ideal value is calculated with the function *MRP.MRPSimulation.generate\_simulated\_reading*, with the same measurement parameters (magnet type, dimensions, sensor distance) as they correspond to the mechanical structure of the used hardware sensor ??.

If the alternative filter algorithm from chapter *Alternative Filter Algorithm Implementation* 5.3.1 is executed here, the same result is returned if the magnet measurement with Identification Number (ID) 5:0 is used as the reference magnet.

The filter algorithm implemented by the user is thus successfully executed using the user-programmable pipeline. The calculation result is successfully verified using raw measurement data and the final result of the algorithm.

# 6 Evaluation

In the previous chapter *Usecase Evaluation 5* it is shown that the implementation of the hardware and software framework for various magnetic field sensors is successfully implemented.

In addition, the basic application by the user is demonstrated based on an example. In this way is possible to systematically characterise magnets from the software and readout hardware side by means of data acquisition, storage and analysis.

After discussing the developed hardware and software components in particular, this chapter will answer the question of whether the selected sensors meet the requirements:

- Measure a wide range of different permanent magnets with regard to their systematic field strength
- Automated measurement of the homogeneity of Halbach rings with an accuracy of less than  $1000\text{ppm}$

These questions are answered in the following, as a basic readout and analysis functionality platform had to be created first and thus an automated sensor characterisation can be performed.

## 6.1 Sensors for Evaluation

The developed framework is directly compatible with a variety of magnetic field sensors without modifications, including those listed in the table 2.1.

Table 6.1: Digital magnetic field sensors characterised for evaluation

	TLV493D-A1B6	MMC5603NJ
Readout-Axis	3D	3D
Temperature-Sensor	yes	yes
Resolution [uT]	98	0.007
Range [mT]	$\pm 130.0$	$\pm 3$
Background-Noise [uT]	100	0.2

For this evaluation, the sensors listed in the table 6.1 were used for sensor characterisation. The additional column for the *Background-Noise* is taken from the respective data sheets of the sensors and will be verified in the later *Background-Noise* measurement 6.3.

This selection is made for the following reasons:

The developed framework is directly compatible with a variety of magnetic field sensors without modifications, including those listed in the table. For this evaluation, the sensors listed in the table were used for sensor characterisation. This selection is made for the following reasons:

- Availability of ready to use development boards
- Specifications correspond to the application areas
- Availability for testing

It is possible to carry out the sensor characterisation shown here for other compatible sensors using the same procedure. Pre-configured measurements 4.1 and analysis pipelines 4.2 are available for this purpose are packaged with library.

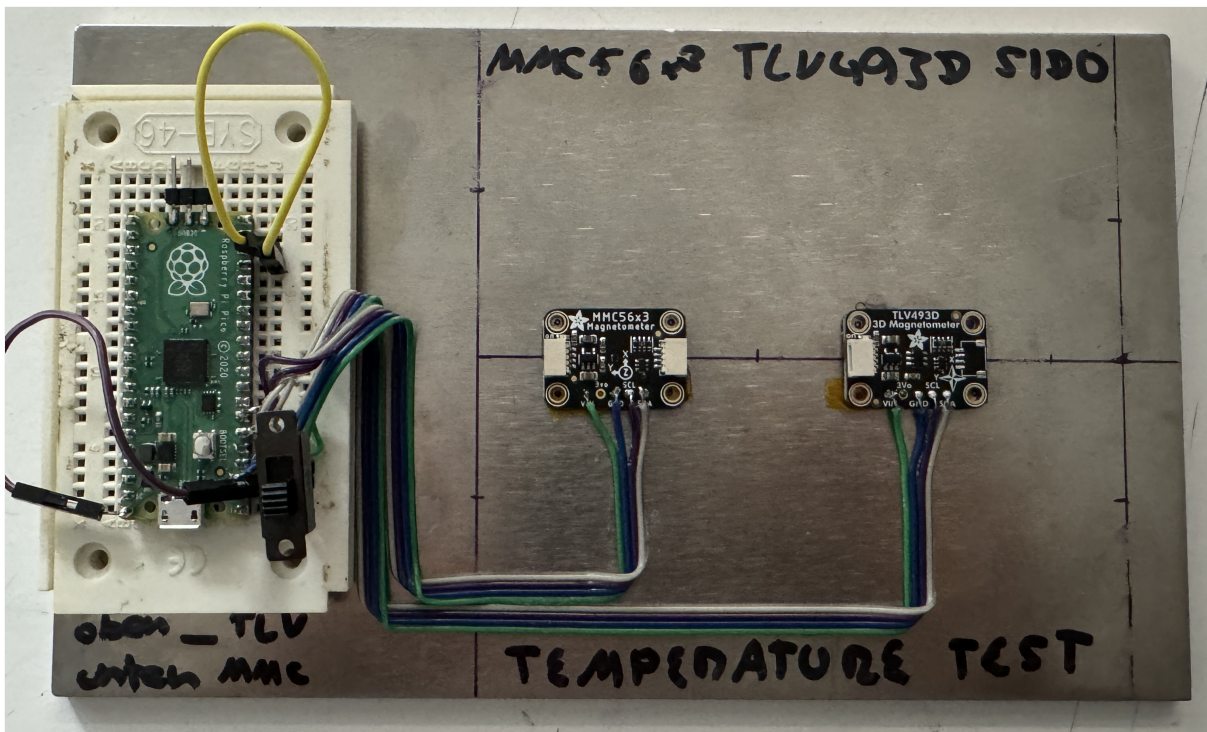


**Figure 6-1:** Sensor evaluation platform with TLV493D and MMC5603 sensors placed with thermal conductive glue on an aluminium baseplate

## 6.2 Evaluation Sensor Setup

The sensor platform used here is an adapted version of the *1D: Single Sensor 2.5.1* sensor platform. The sensors to be measured were fixed together on an aluminium plate with thermally conductive adhesive. This compensates for thermal differences. This is essential for the subsequent temperature deviation tests in order to obtain comparable measurement results.

The setup is placed and pre-wired in the temperature chamber 24 hours before the series of measurements were carried out. The insulated housing of a *Voron 2.4* 3D printer, which has a separately controlled internal heating system, is used as the temperature chamber. To verify the temperature, an additional thermometer *VC-7055BT* is placed on the base plate. A *10mm* thick *PTFE* insulation plate is placed between the floor and the sensor base plate to prevent direct and uneven heating of the base plate by the heated floor.

The graphic 6-1 shows this basic setup, the *Raspberry Pi Pico* shown here is used as the readout hardware, on which the *Unified Sensor Firmware* is running. With additional connected switch, its possible to isolate or select a sensor or both sensors to be queried from the firmware.

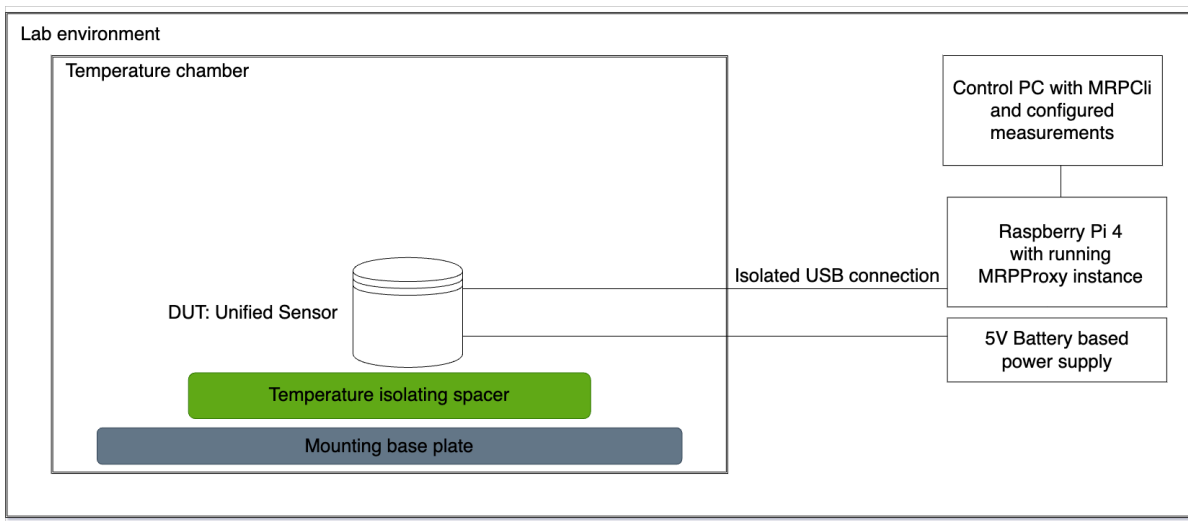


Figure 6-2: Sensor evaluation setup for noise measurements

A separate battery powered supply is used as low-noise power supply for the sensors boards. An *Raspberry Pi 4* is used as the host computer, which is connected to the sensors via a *Hailege ADUM3160* USB isolator and is placed outside the temperature chamber.

For the software setup, *MRPCli* 4.1 is used to control and record the measurement series, with the functions of the *MRPDataVisualisation* 3.4.5 and *MRPAnalysis* 3.4.4 packages from the library 3 being used for subsequent evaluation. The recorded measurement series are automatically analysed using the *Programmable-Data Processing Pipeline* 4.2 and the results are visualised.

## 6.3 Sensor Characterisation: Background-Noise

Measuring the noise in a magnetic field sensor requires a precise procedure and a special measurement setup. First, the magnetic field sensor is placed in a quiet environment to minimize external field interference. The temperature chamber for all noise tests is set to  $\mu_{trev}=21.0^\circ$  and the sensors are placed 24 hours before the measurement run in the final measurement configuration inside of the chamber.

The procedure begins with the acquisition of the baseline by operating the sensor without external magnetic fields. For this purpose, a sample size of  $N=10000$  measured values is recorded for the baseline measurement.

The output signal of the sensor is then continuously measured and recorded. It is important to carry out the measurement over a sufficiently long period of time in order to record both short-term and long-term fluctuations. For this purpose,  $N=2000$  further measured values were taken with a trigger and readout rate of one measurement per second.

In order to quantify the noise, the Standard deviation (SD) of the signal is calculated. These parameters provide information about the variation of the signal over time and therefore about the sensor background noise.

The following figure **6-3** shows the measured values of these sensors. In the following, these are analysed for each sensor examined.

The following data is shown in the plots:

- Plot of the raw data of the sensor
- Plot of the sensors internal temperature sensor
- Background noise level with reference to the initial baseline
- Histogram of the background noise level

The table 6.2 lists the measured values that were extracted from the measurement data of the sensors **6-3**. These measured values are categorised below.

Table 6.2: Sensor noise evaluation results

Symbol	TLV493D	MMC5603NJ	Unit	Description
$\mu_{nl}$	0.79	0.00	%	Mean noise level
$\sigma_{nl}$	0.76	0.00	%	SD noise level
$\mu_{rv}$	157.23	-50.39	$\mu\text{T}$	Mean sensor value (Baseline)
$\sigma_{rv}$	172.00	0.20	$\mu\text{T}$	SD sensor value
$\mu_t$	20.68	19.40	$^{\circ}\text{C}$	Mean sensor temperature
$\sigma_t$	0.53	0.00	$^{\circ}\text{C}$	SD sensor temperature

Symbol	TLV493D	MMC5603NJ	Unit	Description
$\mu_{trev}$	21.0	21.0	°C	Ambient temperature

### 6.3.1 Sensor Temperature Analysis

The temperature stability of the *TLV493D* with a mean value of  $20.68^{\circ}\text{C}$  and a SD of  $\sigma_t=0.53^{\circ}\text{C}$  indicates a consistent trend. This implies a constant tendency. The close grouping of the measured values around the mean value indicates good stability. The confidence interval is expected to be between  $20.15^{\circ}\text{C}$  and  $21.21^{\circ}\text{C}$ , which indicates a stable and consistent temperature measurement. This result is more noisy compared to the temperature stability of the *MMC5603*.

Both sensors provide an offset to the measured chamber temperature  $\mu_{trev}$ .

With an additional measurement run with a different temperature setting of  $30.0^{\circ}\text{C}$ , the measured temperature deviations and offsets remains constant.

The sensor internal temperature sensors of both tested sensors are suitable to perform an ambient temperature compensation of measured values and calibration of the sensor. This is considered in section *Temperature Sensitivity ??*.

It is recommended, however, to use a separate temperature sensor when using the *TLV493D* or to use a suitable averaging of the temperature and measured values in order to perform temperature compensation.

### 6.3.2 Raw Sensor Data Analysis

In the raw data plot, as well as its mean value  $\mu_{rv}$  of both sensors, an offset can also be recognised, which is dependent on the ambient conditions. For verification, a reference measurement of the environment is carried out with the calibrated *Voltcraft GM70* Telsameter next to the sensor IC. This provides a *real* baseline value of  $\mu_{rev}=-21\mu\text{T}$ .

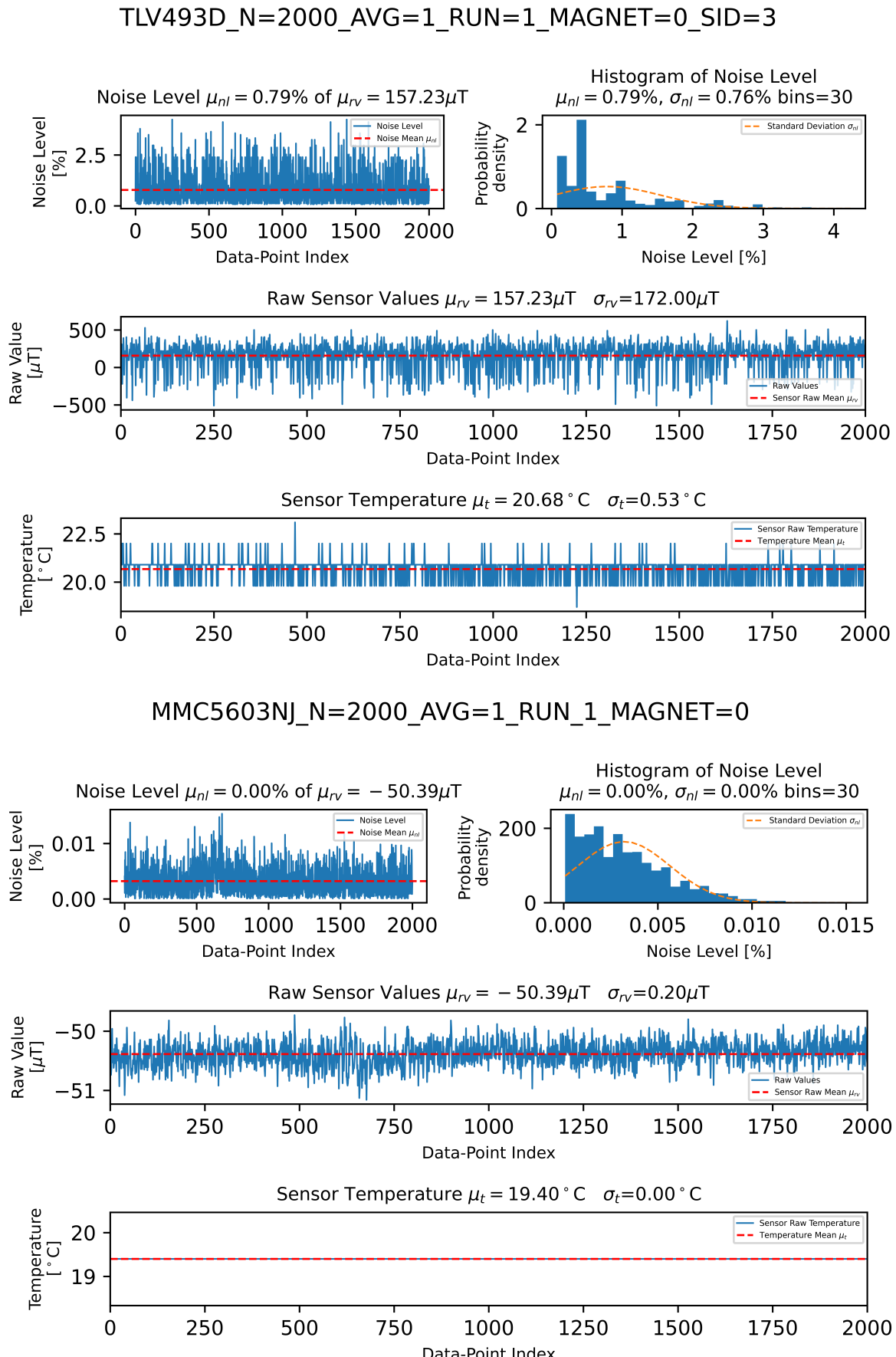


**Figure 6-3:** Sensor noise evaluation results for TLV493D and MMC5603NJ with N=2000 samples and no averaging

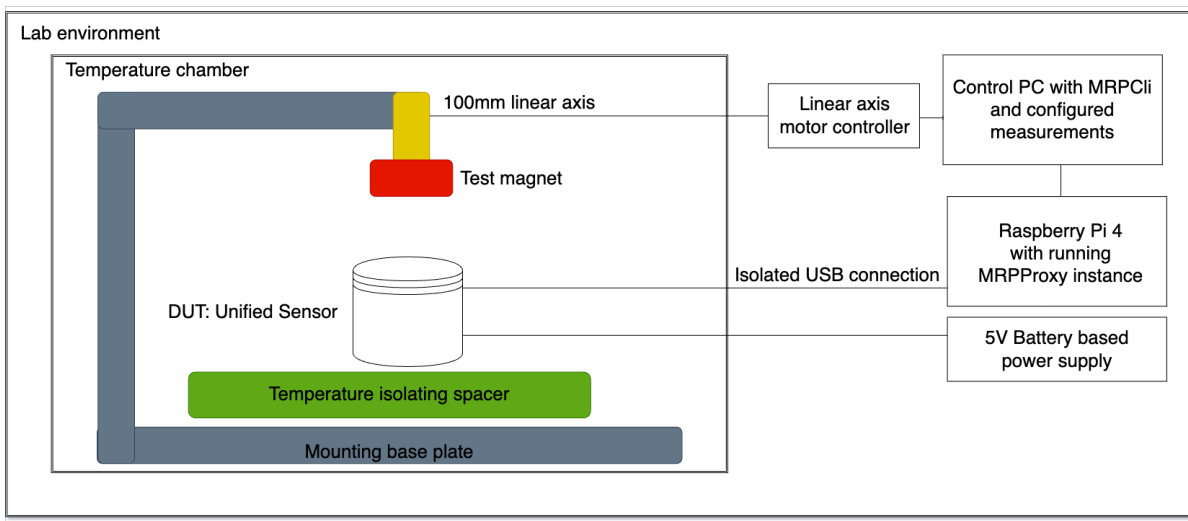


Figure 6-4: Sensor evaluation setup for linearity measurements

## 6.4 Sensor Characterisation: Linearity

The sensor linearity of a magnetic field sensor describes the ability of the sensor to provide a proportional linear response to changes in the magnetic field without non-linear distortions. This means that the output signals of the sensor vary directly proportional to the input magnetic fields without deviations or distortions and is therefore an important indicator for measurements of fields at different distances or objects.

This is achieved here by means of an additional linear axis installed above the sensor setup. A holder for an *N45 12x12x12mm* magnet is attached to the end effector of this axis, which can thus be moved at different distances above the respective sensor IC. The ambient temperature is set to  $\mu_{trev}=21.0^\circ$  in the measurement runs and thus corresponds to the same conditions as in the *Background-Noise6.3* setup.

The figure 6-4 shows this updated measurement setup with the added components. To control the linear axis, an additional motion controller of the type *SKR-Pico* placed outside the temperature chamber is required, which can be controlled via a network interface.

### 6.4.1 Measurement Setup

After the sensor baseline has been determined with  $N=10000$  samples, the magnet is inserted into the holder. The linear axis is moved by the user until it is maximally

saturated. With the *TLV493D*, this corresponds to  $250.000\mu\text{T}$  and below in low resolution mode. *MCC5603NJ* around  $3000\mu\text{T}$ . This ensures that the linearity is determined over the entire measuring range.

#### **6.4.2 Measurement Run**

The measurement run is then started using a script. The user defines the path to be travelled by the linear axis. The complete range of *120mm* in *1mm* steps is selected here. The following automated process then runs as follows:

1. Move the linear axis upwards by the selected distance
2. De-energise the axis motor
3. Create measurement using *MRPCli* with  $N=2000$  data points per reading
4. Export reading to filesystem with current linear axis position in meta-data and filename

#### **6.4.3 Linearity Analysis**

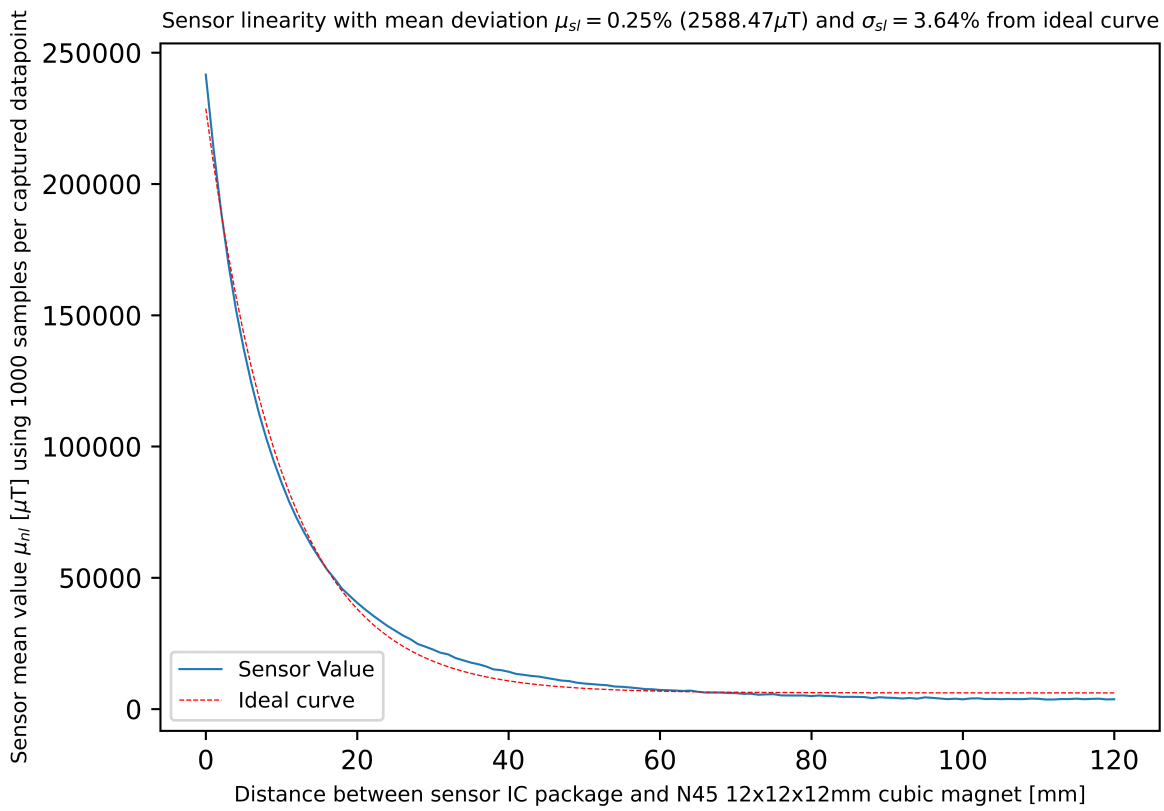
After the measurements were exported, they were analysed for linearity using *MRPAnalysis 3.4.4* functions.

The figure 6-5 shows the visual representation of linearity as a plot. The distance from the magnet to the sensor is plotted in *mm* on the x-axis. The measured value of the sensor is plotted on the y-axis. This is not directly comparable for both plots, as the sensors have different measuring ranges. To ensure comparability, the ideal curve is determined. In order to be able to make quantifiable statements about the measurement results, the mean and SD deviation of these two curves is determined.

For both sensors, the deviation is less than 1% over the entire resolution. With the *MCC5603NJ* this is on average only 0.04%. With the *TLV493D*, however, the SD is 3.64%, for which the deviations at the end in particular (with field strengths towards zero) are decisive. The previously performed *Background-Noise 6.3* characterisation shows that the linearity deviation here is due to the sensitivity of the sensor.

In general, the measured values correspond to the data sheet specifications of both sensors, which specify a value of 5%. It is also possible to calculate these small deviations

Linearity of TLV493D using 120 samples over an distance of 120mm



Linearity of MMC5603NJ using 120 samples over an distance of 120mm

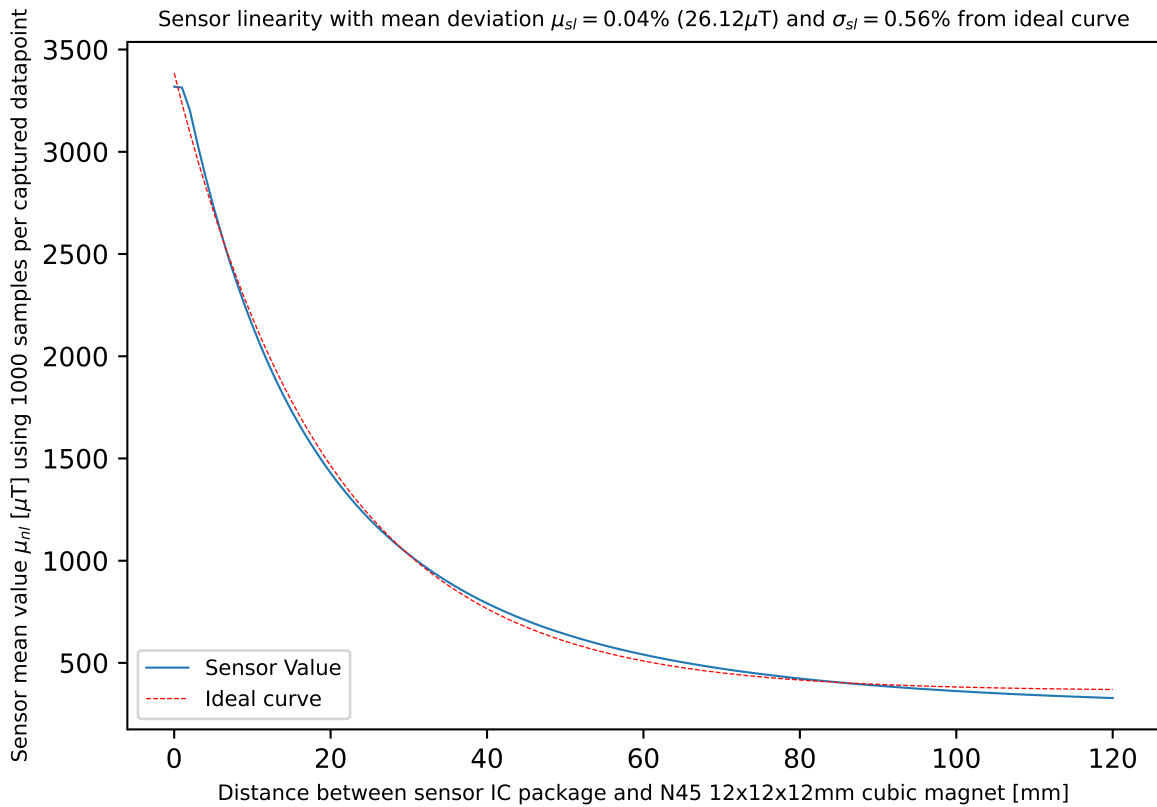


Figure 6-5: Sensor linearity evaluation results for TLV493D and MMC5603NJ

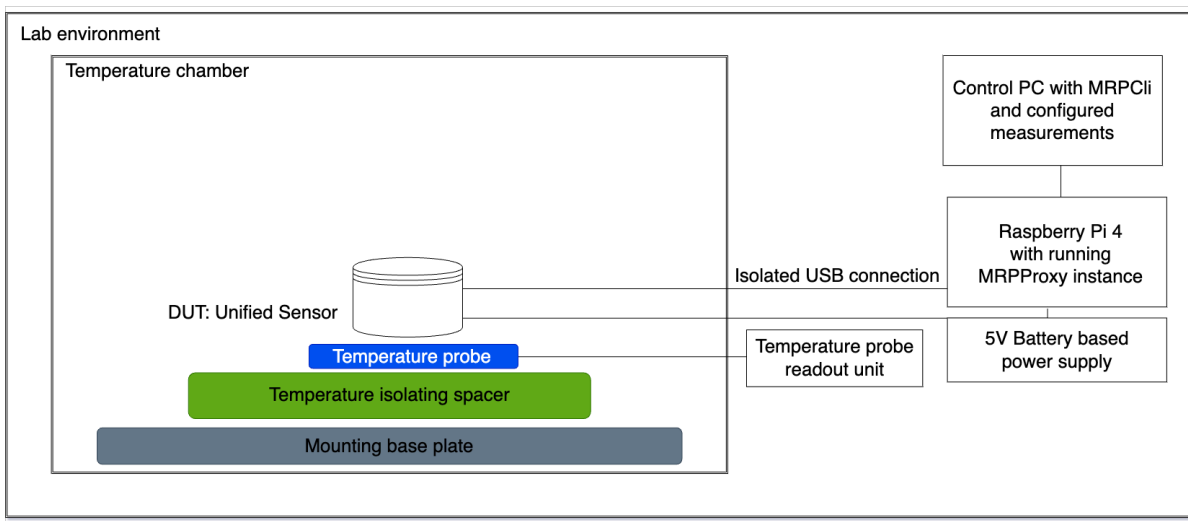


Figure 6-6: Sensor evaluation setup for temperature sensitivity measurements

using curve fitting methods. Suitable functions are implemented in the library.

## 6.5 Sensor Characterisation: Temperature Sensitivity

The temperature sensitivity of magnetic field sensors describes how sensitively the sensors output is sensitive to temperature changes. It is important to ensure that temperature fluctuations do not affect measurement accuracy. A low temperature sensitivity reduces errors due to temperature changes. An accurate temperature sensitivity characteristic is therefore crucial for subsequent precise magnetic field measurements.

As the temperature sensor *TLV493D* in particular produced very different results in the previous measurements, an additional temperature sensor is attached to the sensor circuit board for this measurement. The figure 6-6 shows these modifications in detail. These changes makes it possible to accurately determine the sensors IC temperature. The temperature measuring device *VC-7055BT* can be analysed using a PC interface. The controller of the temperature chamber can also be programmed via a PC interface and a target temperature can be specified.

With this setup, it is possible to automatically acquire measured values from the sensors under controlled temperature conditions.

The same procedure is used as for the *Linearity 6.4* measurement, except that instead of moving the linear axis, the temperature of the temperature chamber is systematically

increased from 20° to 50°. Between each of these temperature changes, the system is given a waiting time of 30 minutes after reaching the target temperature.

The field of permanent magnets is very temperature-dependent and can lose its magnetisation at higher temperatures (typically  $>=80^\circ$  for non-high-quality type N magnets [14]). The temperature range is selected so that it is within a sufficient range for the application.

### **6.5.1 Temperature Sensitivity Analysis**

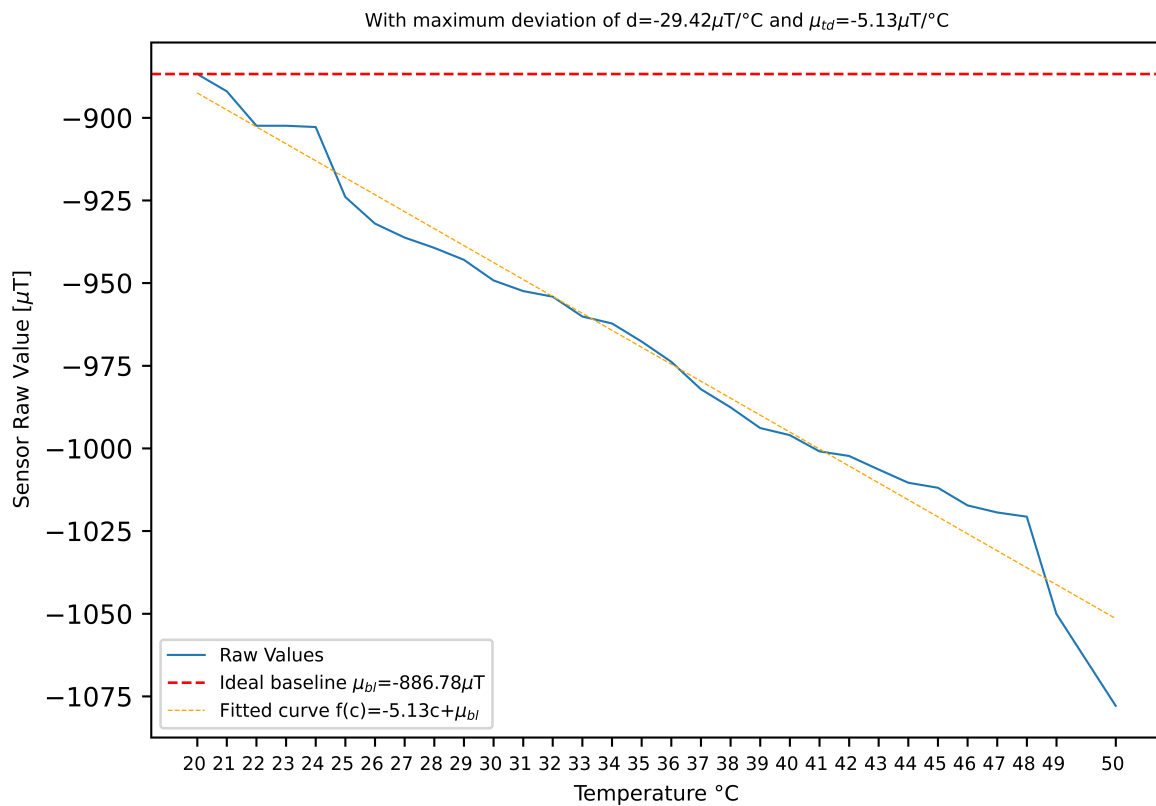
The figure 6-7 shows the measured data as a plot with the temperature measured by the measuring devices on the X-axis and the sensor measured value on the Y-axis. The ideal baseline is also shown as a red line. It can be seen that the *MMC5603NJ* shows a straight-line drop in the measured field strength with increasing temperatures. However, this is very constant with a value of  $-2 \mu T / {}^\circ C$  and is therefore predictable.

The graph of the *TLV493d* is significantly steeper with a gradient of  $-5.13 \mu T / {}^\circ C$ , and it is also not as linear as the *MMC5603NJ*; there are clear jumps in the gradient. However, the total change between the temperature regions of  $175 \mu T$  is less than that of the *MMC5603NJ* with  $70 \mu T$ , if the total measurement range of the sensors is also taken into account.

In the evaluation (see figure 6-7), a linear function was also calculated using curve fitting to determine the temperature coefficients of the sensors. This makes it possible to compensate these deviations based on the ambient temperature during the software calibration.

## **6.6 Result Analysis**

Temperature sensitivity of TLV493D using N=1 samples per increased °C



Temperature sensitivity of MMC5603NJ using N=1 samples per increased °C

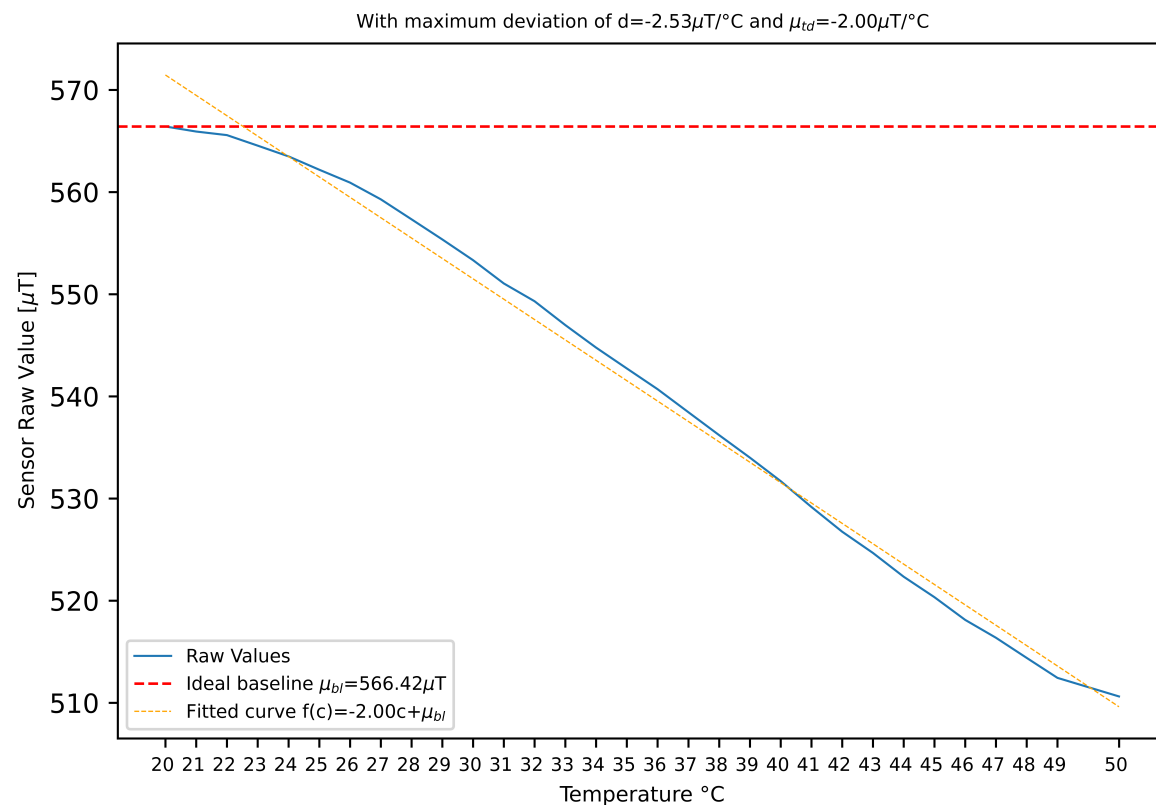


**Figure 6-7:** Sensor temperature sensitivity evaluation results for TLV493D and MMC5603NJ

Table 6.3: Overview of all characterised sensor properties

Symbol	TLV493D	MMC5603NJ	Unit	Description
$\mu_{nl}$	0.79	0.00	%	Mean noise level
$\sigma_{nl}$	0.76	0.00	%	SD noise level
$\mu_{rv}$	157.23	-50.39	$\mu\text{T}$	Mean sensor value (Baseline)
$\sigma_{rv}$	172.00	0.20	$\mu\text{T}$	SD sensor value
$\mu_t$	20.68	19.40	$^{\circ}\text{C}$	Mean sensor temperature
$\sigma_t$	0.53	0.00	$^{\circ}\text{C}$	SD sensor temperature
$\mu_{trev}$	21.0	21.0	$^{\circ}\text{C}$	Ambient temperature
$\mu_{sl}$	0.25	0.04	%	Mean sensor linearity deviation
$\sigma_{sl}$	3.64	0.56	%	SD sensor linearity
$\mu_{td}$	-1.99	-5.13	$\mu\text{T} / ^{\circ}\text{C}$	Mean sensor temperature coefficients

Table 6.3 shows a summary of all recorded and analysed measured values of the two characterised sensors *TLV493D* and *MMC5603NJ*. It can be clearly seen that these differ significantly by a factor of  $x10$ .

The *TLV493D* performs seriously in the Senosr Noise measurement and also performs worse than specified in the data sheet ( $98\mu\text{T}$  instead of  $175\mu\text{T}$ ), but the large measuring range, which fulfils the required specifications from chapter *Research Question 1.4*, must be taken into account here, which is not met by the *MMC5603NJ*.

The *MMC5603NJ* can be used directly without additional software calibration for measuring permanent magnets. Even without additional measurement averaging, very precise measurement results can be achieved, which achieve a measurement accuracy of less than *1000ppm*.

However, due to the limited measuring range of  $\pm 3mT$ , direct measurement of stronger magnets is not possible. The *N45 12x12x12mm* magnets used in the application typically have a field strength of around  $100mT$  at a distance of  $10mm$ .

The *TLV493D*, on the other hand, is able to measure these directly, but does not achieve the required accuracy due to strong noise and steep temperature coefficients.

In the following chapter, recommendations for action are defined, which were derived from the analysis results.

### **6.6.1 Recommendation for Action**

- folgendes setup wird für eine vermessung nach der sensor auswertung emholen:
- temperaturkomensation sowie linearitäts kompensation mit separaten temperatur sensor

are they suitable for <1000(+ppm) ?

- <https://onlinelibrary.wiley.com/doi/epdf/10.1002/mrm.28396>
- 27cm / 50mT bore
- nmr probes for better results
- mit software calibrierung ist es möglich vermutlich möglich sowie mittelung ist es möglich auch mit dem tlv493d kanpp unter die 50uT zu kommen
- mess durchläufe mit ist es mögloch von 175uT nach 70uT zu kommen mit avg=20 kommt man auf 45
- sollte ein geeigneter ersatzsensor gefunden werden
- beide sensoren sind jedoch durch chrakterisierung von permanentmagneten ge-eignet
- beim tlv493d ist es möglich absolut werte zu erfassen.

- beim mmc ist es möglich relativ magnete untereinander zu vergleichen

# 7 Conclusion and Discussion

## 7.1 Conclusion

This work describes the development of a universal Python library that is used to efficiently process data from magnetic field sensors from acquisition to analysis. In order to ensure a practical application and to give users the opportunity to directly acquire their own magnetic field data, cost-effective and easily reproducible hardware is also developed.

The hardware is based on widely used magnetic field sensors and low-cost microcontrollers, which enables an easily expandable and applicable solution for measuring magnets with repeatable accuracy.

A particular focus is placed on expandability by the user. Interchangeable modules allow the user to develop their own analysis algorithms without having to redesign everything from scratch.

This extensibility and customisability is successfully demonstrated during the evaluation. This underlines the performance of the developed framework and shows that it is not only effective in the processing of magnetic field sensor data, but also offers a flexible platform for the implementation of user-specific analyses.

## 7.2 Outlook

A solid foundation has been built in this version of the framework, which contains all the necessary functions and is ready for immediate use. During development, particular emphasis is placed on comprehensive documentation to make it easier to get

started. Together with examples for various usecases, a user can quickly evaluate the framework.

However, it should be noted that the framework has already been released with its first stable version, but extensions and improvements are still necessary. The stable version distributed via the package registry is well suited for the intended purpose. All tests and evaluations took place under normal conditions, especially for the developed hardware sensors, as the MRP library works successfully with the measurement data.

On the software side, the focus is on integration for the support of more professional measuring devices. Only in this way is it possible to evaluate and improve the sensor hardware and quantify the measurement results.

To summarise, it can be said that a solid software framework has been created that can be used directly for the intended purpose. It provides a suitable working foundation, but can be further developed by integrating professional measurement devices to enable a more comprehensive evaluation and improvement of the sensor hardware.

# Bibliography

- [1] ARNOLD, Thomas C. ; FREEMAN, Colbey W. ; LITT, Brian ; STEIN, Joel M.: Low-field MRI: Clinical promise and challenges. In: *J. Magn. Reson. Imaging* 57 (2023), Januar, Nr. 1, S. 25–44
- [2] BENJAMIN MENKÜC, Thomas O. Lukas Winter W. Lukas Winter: *HalbachMRI-Designer - Create a Halbach MRI Magnet from parametric definitions.* <https://github.com/menkueclab/HalbachMRIDesigner>. Version: 01.01.2024
- [3] BLÜMLER, Peter ; CASANOVA, Federico: *CHAPTER 5: Hardware developments: Halbach magnet arrays.* 2016. – 133–157 S. <http://dx.doi.org/10.1039/9781782628095-00133>. – <http://dx.doi.org/10.1039/9781782628095-00133>. – ISBN 978–1–84973–915–3
- [4] DEVELOPERS, Sphinx: *Sphinx makes it easy to create intelligent and beautiful documentation.* <https://www.sphinx-doc.org/en/master/>. Version: 01.01.2024
- [5] Docs, Inc Read t.: *MagneticReadoutProcessing - ReadTheDocs.* <https://magneticreadoutprocessing.readthedocs.io/en/latest/index.html>. Version: 01.01.2024
- [6] Docs, Inc Read t.: *ReadTheDocs - Build, host, and share documentation, all with a single platform.* <https://readthedocs.com>. Version: 01.01.2024
- [7] FOUNDATION, Python S.: *MagneticReadoutProcessing - PyPi.* <https://pypi.org/project/MagneticReadoutProcessing/>. Version: 01.01.2024
- [8] FOUNDATION, Python S.: *PyPi - The Python Package Index (PyPI) is a software directory for the Python programming language.* <https://pypi.org>. Version: 01.01.2024

## Bibliography

---

- [9] FOUNDATION, Python S.: *Python Docs - globals*. <https://docs.python.org/3/library/functions.html#globals>. Version:01.01.2024
- [10] FOUNDATION, Python S.: *Python Docs - heapq*. <https://docs.python.org/3/library/heappq.html>. Version:01.01.2024
- [11] FOUNDATION, Python S.: *Python Enhancement Proposals - Docstring Conventions*. <https://peps.python.org/pep-0257/>. Version:01.01.2024
- [12] GEERLING, Jeff: *PTP and IEEE-1588 hardware timestamping*. <https://www.jeffgeerling.com/blog/2022/ptp-and-ieee-1588-hardware-timestamping-on-raspberry-pi-cm4>. Version:01.01.2024
- [13] GITHUB, Inc.: *Github Actions - Automate your workflow from idea to production*. <https://github.com/features/actions>. Version:01.01.2024
- [14] GMBH, Magna-C: *Magnet - Curie-Temperature*. <https://www.magna-c.com/der-magnet/einsatztemperatur>. Version:01.01.2024
- [15] HALBACH, Klaus.: Design of permanent multipole magnets with oriented rare earth cobalt material. In: *Nuclear Instruments and Methods* 169 (1980), 1-10. <https://api.semanticscholar.org/CorpusID:53486791>
- [16] HARRIS, Charles R. ; MILLMAN, K. J. ; WALT, Stéfan J. ; GOMMERS, Ralf ; VIRTANEN, Pauli ; COURNAPEAU, David ; WIESER, Eric ; TAYLOR, Julian ; BERG, Sebastian ; SMITH, Nathaniel J. ; KERN, Robert ; PICUS, Matti ; HOYER, Stephan ; KERKWIJK, Marten H. ; BRETT, Matthew ; HALDANE, Allan ; RÍO, Jaime F. ; WIEBE, Mark ; PETERSON, Pearu ; GÉRARD-MARCHANT, Pierre ; SHEPPARD, Kevin ; REDDY, Tyler ; WECKESSER, Warren ; ABBASI, Hameer ; GOHLKE, Christoph ; OLIPHANT, Travis E.: Array programming with NumPy. In: *Nature* 585 (2020), September, Nr. 7825, 357–362. <http://dx.doi.org/10.1038/s41586-020-2649-2>. – DOI 10.1038/s41586-020-2649-2
- [17] HORI, Masaaki ; HAGIWARA, Akifumi ; GOTO, Masami ; WADA, Akihiko ; AOKI, Shigeki: Low-field magnetic resonance imaging: Its history and renaissance. In: *Invest. Radiol.* 56 (2021), November, Nr. 11, S. 669–679
- [18] KINTEL, Marius: *OpenSCAD - The Programmers Solid 3D CAD Modeller*. <https://openscad.org>

## Bibliography

---

//openscad.org. Version:01.01.2024

- [19] KREKEL, Holger ; TEAM pytest-dev: *pytest: helps you write better programs.* <https://docs.pytest.org/en/7.4.x/>. Version:01.01.2024
- [20] NITZ, Wolfgang R. ; KRAMME, Rüdiger (Hrsg.): *Magnetresonanztomographie (MRT) – Komponenten und Methoden.* Berlin, Heidelberg : Springer Berlin Heidelberg, 2016. – 1–22 S. [http://dx.doi.org/10.1007/978-3-662-45538-8\\_18-1](http://dx.doi.org/10.1007/978-3-662-45538-8_18-1). <http://dx.doi.org/10.1007/978-3-662-45538-8> – ISBN 978–3–662–45538–8
- [21] OCHSENDORF, Marcel: *VoltcraftGM70 REST Interface.* <https://github.com/RBEGamer/VoltcraftGM70Rest>. Version:01.01.2024
- [22] O'REILLY, T ; TEEUWISSE, W M. ; WEBB, A G.: Three-dimensional MRI in a homogenous 27 cm diameter bore Halbach array magnet. In: *J. Magn. Reson.* 307 (2019), Oktober, Nr. 106578, S. 106578
- [23] O'REILLY, Thomas: *HalbachOptimisation - An implementation of a genetic algorithm to optimise the homogeneity of a Halbach array by varying the ring diameters along the length of the Halbach cylinder.* <https://github.com/LUMC-LowFieldMRI/HalbachOptimisation>. Version:01.01.2024
- [24] O'REILLY, Thomas ; TEEUWISSE, Wouter M. ; GANS, Danny de ; KOOLSTRA, Kirsten ; WEBB, Andrew G.: In vivo 3D brain and extremity MRI at 50 mT using a permanent magnet Halbach array. In: *Magn. Reson. Med.* 85 (2021), Januar, Nr. 1, S. 495–505
- [25] ORTNER, Michael ; BANDEIRA, Lucas Gabriel C.: Magpylib: A free Python package for magnetic field computation. In: *SoftwareX* 11 (2020), S. 100466
- [26] PETER BLUEMLER, Helmut S.: Practical Concepts for Design, Construction and Application of Halbach Magnets in Magnetic Resonance. In: *Applied Magnetic Resonance* (2023), 05, S. 2522. <http://dx.doi.org/10.1007/s00723-023-01602-2>. – DOI 10.1007/s00723–023–01602–2
- [27] SOLTNER, H. ; BLÜMLER, P.: Dipolar Halbach magnet stacks made from identically shaped permanent magnets for magnetic resonance. In: *Concepts in Magnetic Resonance Part A* 36A (2010), Nr. 4, 211-222. <http://dx.doi.org/https://doi.org/10.1002/cmr.a.20165>. – DOI <https://doi.org/10.1002/cmr.a.20165>

- [28] VOS, Bart de ; REMIS, Rob F. ; WEBB, Andrew G.: An integrated target field framework for point-of-care halbach array low-field MRI system design. In: *MAGMA* 36 (2023), Mai, Nr. 3, S. 395–408
- [29] WENZEL, Konstantin ; ALHAMWEY, Hazem ; O'REILLY, Tom ; RIEMANN, Layla T. ; SILEMEK, Berk ; WINTER, Lukas: B0-Shimming Methodology for Affordable and Compact Low-Field Magnetic Resonance Imaging Magnets. In: *Frontiers in Physics* 9 (2021). <http://dx.doi.org/10.3389/fphy.2021.704566>. – DOI 10.3389/fphy.2021.704566. – ISSN 2296–424X
- [30] WICKENBROCK, Arne ; ZHENG, Huijie ; CHATZIDROSOS, Georgios ; SHAJI REBEIRRO, Joseph ; SCHNEEMANN, Tim ; BLÜMLER, Peter: High homogeneity permanent magnet for diamond magnetometry. In: *Journal of Magnetic Resonance* 322 (2021), Januar, 106867. <http://dx.doi.org/10.1016/j.jmr.2020.106867>. – DOI 10.1016/j.jmr.2020.106867. – ISSN 1090–7807

# List of Figures

1-1	Example Hallbach ring with cutouts for eight magnets . . . . .	5
2-1	Mechanical components for the 1D sensor using 3D printed parts . . . . .	17
2-2	1D sensor schematic and circuit board . . . . .	18
2-3	Unified sensor firmware simplified program structure . . . . .	19
2-4	Sensors CLI . . . . .	21
2-5	Query sensors b value using CLI . . . . .	22
2-6	Multi sensor synchronisation wiring example . . . . .	22
2-7	Unified sensor firmware multi sensor synchronisation procedure . . . . .	25
2-8	Query opmode using CLI . . . . .	25
2-9	1D sensor construction with universal magnet mount . . . . .	26
2-10	Full-Sphere sensor implementation using two Nema17 stepper motors in a polar coordinate system . . . . .	28
2-11	3D plot of an N45 12x12x12 magnet using the 3D fullsphere sensor . . . . .	28
2-12	Voltcraft GM70 teslameter with custom PC interface board . . . . .	30
3-1	MRP library module high level overview . . . . .	32
3-2	MRPlib Proxy Module . . . . .	40
3-3	Example MRP proxy module usage, using two remote PCs . . . . .	40
3-4	Example full sphere plot of an measurement using the MRPVisualisation module . . . . .	50
3-5	Generated Hallbach array with generated cutouts for eight magnets . . . . .	52
4-1	MRP CLI output to configure a new measurement . . . . .	53
4-2	Example measurement analysis pipeline . . . . .	55
4-3	Example result of an step execution tree from user defined processing pipeline . . . . .	57
4-4	Pipeline output files after running example pipeline on a set of readings . . . . .	58
4-5	MRP library test results for different submodules executed in PyCharm IDE . . . . .	58
4-6	MagneticReadoutProcessing library hosted on PyPi . . . . .	60
4-7	MagneticReadoutProcessing documentation hosted on ReadTheDocs . . . . .	63

## List of Figures

---

5-1	Ten numbered test magnets in separate holders . . . . .	65
5-2	MRP evaluation result after execution of the user defined pipeline, using find similar values algorithm . . . . .	70
6-1	Sensor evaluation platform with TLV493D and MMC5603 sensors placed with thermal conductive glue on an aluminium baseplate . . . . .	73
6-2	Sensor evaluation setup for noise measurements . . . . .	74
6-3	Sensor noise evaluation results for TLV493D and MMC5603NJ with N=2000 samples and no averaging . . . . .	77
6-4	Sensor evaluation setup for linearity measurements . . . . .	78
6-5	Sensor linearity evaluation results for TLV493D and MMC5603NJ . . .	80
6-6	Sensor evaluation setup for temperature sensitivity measurements . . .	81
6-7	Sensor temperature sensitivity evaluation results for TLV493D and MMC5603NJ . . . . .	83

# List of Tables

2.1	Implemented digital magnetic field sensors . . . . .	16
2.2	Measured sensor readout to processing using host software . . . . .	23
2.3	Build sensors with different capabilities . . . . .	26
3.1	Sensor capabilities merging algorithm . . . . .	43
6.1	Digital magnetic field sensors characterised for evaluation . . . . .	72
6.2	Sensor noise evaluation results . . . . .	75
6.3	Overview of all characterised sensor properties . . . . .	84

# Listings

2.1	CustomSensor-Class for adding new sensor hardware support . . . . .	20
3.1	JSON export structure of an MRPReading based measurement . . . . .	36
3.2	MRPproxy usage to enable local sensor usage over network . . . . .	41
3.3	MRPProxy REST endpoint query examples . . . . .	41
3.4	MRPcli usage example to connect with a network sensor . . . . .	42
3.5	MRPproxy REST enpoiint query examples . . . . .	44
3.6	MRPReading example for setting up an basic measurement . . . . .	45
3.7	MRPHal example to use an connected hardware sensor to store readings inside of a measurement . . . . .	46
3.8	MRPSimulation example illustrates the usage of several data analysis functions . . . . .	47
3.9	MRPAnalysis example code performs several data analysis steps . . . . .	48
3.10	MRPVisualisation example which plots a fullsphere to an image file . . . . .	49
3.11	MRPHalbachArrayGenerator example for generating an OpenSCAD based halbach ring . . . . .	51
4.1	CLI example for configuring a measurement run . . . . .	54
4.2	Example YAML code of an user defined processing pipeline with six stages linked together . . . . .	56
4.3	Example pytest class for testing MRPReading module functions . . . . .	59
4.4	Bash commands to install the MagneticReadoutProcessing library using pip . . . . .	60
4.5	setup.py with dynamic requirement parsing used given requirements.txt	61
4.6	Documentation using Python docstring example . . . . .	62
5.1	Measurement configuration for evaluation measurement . . . . .	66
5.2	User implemented custom find most similar readings algorithm . . . . .	66
5.3	Modified user implemented custom find algorithm using a reference magnet reading . . . . .	67
5.4	User defined processing pipeline using custom implemented filter algorithm	68
5.5	Bash result log of evaluation pipeline run . . . . .	69